Biogeosciences, 19, 3979–4010, 2022
https://doi.org/10.5194/bg-19-3979-2022

Biogeosciences Open Access EGU

From soil to sea: sources and transport of organic carbon traced by tetraether lipids in the monsoonal Godavari River, India

Frédérique M. S. A. Kirkels[1], Huub M. Zwart[1], Muhammed O. Usman[2,a], Suning Hou[1], Camilo Ponton[3,b], Liviu Giosan[3], Timothy I. Eglinton[2], and Francien Peterse[1]

[1]Department of Earth Sciences, Utrecht University, Utrecht, the Netherlands
[2]Geological Institute, ETH Zürich, Zurich, Switzerland
[3]Geology and Geophysics, Woods Hole Oceanographic Institution, Woods Hole, MA, USA
[a]present address: Department of Physical and Environmental Sciences,
University of Toronto Scarborough, Toronto, Ontario, Canada
[b]present address: Geology Department, Western Washington University, Bellingham, WA, USA

Correspondence: Francien Peterse (f.peterse@uu.nl)

Received: 8 May 2022 – Discussion started: 23 May 2022
Revised: 9 August 2022 – Accepted: 15 August 2022 – Published: 1 September 2022

Abstract. Monsoonal rivers play an important role in the land-to-sea transport of soil-derived organic carbon (OC). However, spatial and temporal variation in the concentration, composition, and fate of this OC in these rivers remains poorly understood. We investigate soil-to-sea transport of soil OC by the Godavari River in India using glycerol dialkyl glycerol tetraether (GDGT) lipids in soils, river suspended particulate matter (SPM), and riverbed sediments, as well as in a marine sediment core from the Bay of Bengal. The abundance and composition of GDGTs in SPM and sediments in the Godavari River differs between the dry and wet season. In the dry season, SPM and riverbed sediments from the whole basin contain more 6-methyl branched GDGTs (brGDGTs) than the soils. In the upper basin, where mobilisation and transport of soils is limited due to deficient rainfall and damming, contributions of 6-methyl brGDGTs in SPM and riverbed sediments are relatively high year-round, suggesting that they have an aquatic source. Aquatic brGDGT production coincides with elevated values of the isoprenoid GDGT-0 / crenarchaeol ratio in SPM and riverbed sediments from the upper basin, indicating low-oxygen conditions. In the wet season, brGDGT distributions in SPM from the lower basin closely resemble those in soils, mostly from the north and east tributaries, corresponding to precipitation patterns. The brGDGT composition in SPM and sediments from the delta suggests that soil OC is only effectively transported to the Bay of Bengal in the wet season, when the river plume extends beyond the river mouth. The sediment geochemistry indicates that also the mineral particles exported by the Godavari River primarily originate from the lower basin, similar to the brGDGTs, suggesting that they are transported together. However, river depth profiles in the downstream Godavari reveal no hydrodynamic sorting effect on brGDGTs in either season, indicating that brGDGTs are not closely associated with mineral particles. The similarity of brGDGT distributions in bulk and fine-grained sediments ($\leq 63\,\mu m$) further confirms the absence of selective transport mechanisms. Nevertheless, the composition of brGDGTs in a Holocene, marine sediment core near the river mouth appears substantially different from that in the modern Godavari basin, suggesting that terrestrial-derived brGDGTs are rapidly lost upon discharge into the Bay of Bengal and/or overprinted by marine in situ production. The large change in brGDGT distributions at the river–sea transition implies that this zone is key in the transfer of soil OC, as well as that of the environmental signal carried by brGDGTs from the river basin.

Published by Copernicus Publications on behalf of the European Geosciences Union.

1 Introduction

Fluvial land-to-sea transport of organic carbon (OC) plays a key role in the global carbon cycle (Aufdenkampe et al., 2011; Bianchi et al., 2011; Galy et al., 2015; Ward et al., 2017). The burial of river-exported OC in marine sediments results in the long-term sequestration of photosynthetically fixed CO_2 from the atmosphere (Hedges an Keil, 1995; Hedges et al., 1997; Leithold et al., 2016). On land, soils are the most important OC pool (1500–2400 Gt), as its size exceeds the atmospheric and biotic inventories (> 2.2 and 2.3 times, respectively) (Friedlingstein et al., 2020). Soil organic carbon (SOC) is continuously mobilised by erosion processes and transferred into rivers, where it forms a key component of fluvial OC (Holtvoeth et al., 2005; Tao et al., 2015). Rivers were long considered "pipelines" or "passive channels" where SOC remains unchanged during transport downstream and represents an integration of the whole river basin (Cole et al., 2007). However, it appears that only a fraction (30 %–50 %) of the SOC that enters a river ultimately reaches the ocean (Cole et al., 2007; Battin et al., 2009; Aufdenkampe et al., 2011; Bianchi et al., 2011; Ward et al., 2017) and that its composition can be highly altered during transport (Hedges, 1992; Hedges et al., 1997).

The pathway of SOC through a river basin, i.e. where, when, and to what extent it is mobilised, processed enroute, or transferred downstream and exported to the ocean, is determined by a combination of physical and biogeochemical processes along the soil–river–ocean continuum (Cole et al., 2007; Battin et al., 2009; Aufdenkampe et al., 2011; Butman and Raymond, 2011; Regnier et al., 2013; Ward et al., 2017). For example, the stability of SOC during transport, and thus its potential for final preservation in marine sediments, can be influenced by the mode of transport: in free (uncomplexed) form or associated with mineral surfaces (e.g. organo-mineral complexes) due to differences in transport efficiency, sinking velocity, and physical protection against microbial and oxidative attack (Mayer, 1994; Keil et al., 1997; Blattmann et al., 2019; Hemingway et al., 2019). Changes in the sourcing of SOC from specific parts of a basin corresponding to temporal variations in rainfall patterns are known to influence OC that is finally exported to the ocean (e.g. Galy et al., 2008; Hemingway et al., 2017; Menges et al., 2020). In addition, hydrodynamic particle sorting can cause stratification of sediment loads with depth and can thus affect bulk OC transport (Galy et al., 2008; Bouchez et al., 2011, 2014), although influences on specific OC components may vary (Freymond et al., 2018a). Notably, terrigenous OC that is moved through a river basin can be a composite of soil-derived (pedogenic) and rock-derived (petrogenic) OC, with in situ aquatic productivity as additional OC source (e.g. Eglinton et al., 2021). Disentangling the sources of river-transported OC is difficult using bulk measurements, and as a result, the timescales and mechanisms (quantitative and qualitative) of transport, as well as the composition of the OC that is finally discharged to the ocean, remain elusive for many river systems. Although lipid biomarkers represent only a small part of the total OC, their source- or environment-specific signature renders them as promising tracers in river systems (e.g. Eglinton et al., 2021).

Over the past decade, bacterial membrane lipids, so-called branched glycerol dialkyl glycerol tetraethers (brGDGTs), have been used to trace soil organic matter inputs into rivers and continental margins (e.g. Hopmans et al., 2004; Weijers et al., 2009a; Kim et al., 2012; Zell et al., 2013a, b; Kirkels et al., 2020a; Märki et al., 2020). Branched GDGTs occur globally in soils and peats and can vary in the number (4–6) and position of methyl branches (5/5′ or 6/6′, defined as 5-methyl and 6-methyl) attached to linear C_{28} alkyl chains, as well as the presence of 0–2 cyclopentane moieties (Weijers et al., 2007a; De Jonge et al., 2013, 2014a; Naafs et al., 2017; see figures therein for the molecular structures). Although their exact producer(s) remain(s) largely unknown, the stereochemistry of the glycerol moieties of brGDGTs points toward a bacterial source (Weijers et al., 2006), likely Acidobacteria (Weijers et al., 2009b; Sinninghe Damsté et al., 2011). Iso-diabolic acids, which are considered building blocks of brGDGTs, have been detected in Acidobacteria subdivisions 1, 3, 4, and 6 (Sinninghe Damsté et al., 2014, 2018). Whereas most subdivisions produce iso-diabolic acid with a methylation on the 6/6′ position, 5-methyl iso-diabolic acid appears so far to be exclusively produced by Acidobacteria from subdivision 4 (Sinninghe Damsté et al., 2014, 2018). The identification of Acidobacteria that produce intact brGDGTs was so far limited to two cultured species of subdivision 1 that synthesise brGDGT Ia (Sinninghe Damsté et al., 2011; Halamka et al., 2021), but it cannot be excluded that other species may also produce brGDGTs (Sinninghe Damsté et al., 2018).

The presence of brGDGTs in coastal marine sediments relative to that of crenarchaeol, an isoprenoid GDGT (isoGDGT) produced by marine Thaumarchaeota (Sinninghe Damsté et al., 2002), has been proposed as a proxy to determine the relative contribution of terrestrial OC into a marine environment and is quantified in the branched and isoprenoid tetraether (BIT) index (Hopmans et al., 2004). In addition, brGDGTs in coastal marine sediments have been used to reconstruct paleoenvironmental changes on the nearby land based on the empirical relations between the degree of methylation of 5-methyl brGDGTs (MBT'_{5Me}) and mean annual air temperature (MAAT) and between the degree of cyclisation of branched tetraethers (CBT') as well as the relative abundance of 6-methyl brGDGTs and soil pH found in modern surface soils and peats (Weijers et al., 2007a, b; De Jonge et al., 2014a; Naafs et al., 2017; Dearing Crampton-Flood et al., 2020). The use of these brGDGT proxies assumes that brGDGTs preserved in continental margin sediments have a soil origin and represent a basin-integrated signal. Indeed, the composition of brGDGTs in rivers has been shown to resemble those in soils in upstream catch-

ments (e.g. Kirkels et al., 2020a; Märki et al., 2020). However, in downstream areas, stagnant waters, and periods with low flow, brGDGTs are also produced in rivers (e.g. Yang et al., 2013; Zell et al., 2013a, b, 2014a; De Jonge et al., 2014b, 2015a; Kim et al., 2015; Freymond et al., 2017), which complicates their use as soil-specific tracers. For example, Zell et al. (2013a, b) reported a mismatch between brGDGT distributions in soils and river suspended particulate matter (SPM) from the lower Amazon River in the dry season and attributed this difference to in situ aquatic brGDGT production. In addition, (seasonal) hydroclimate variability may influence the provenance, i.e. source location, within a basin of brGDGTs in a river basin. For example, brGDGT distributions in SPM from the Congo River matched with different areas of the river basin during the year, in response to seasonal changes in rainfall patterns (Hemingway et al., 2017). Further progress on untangling brGDGT sources has been made since De Jonge et al. (2014b) discovered a potential link between the occurrence of 6-methyl brGDGTs and aquatic production in rivers based on predominance of these isomers in SPM of the Yenisei River compared to local soils, likely due to the generally higher pH of river water than most soils. The abundance of 6-methyl brGDGTs relative to 5-methyl isomers can be quantified in the isomer ratio (IR), where higher IR values appear to be indicative of more aquatic production. Following this principle, Guo et al. (2020) determined that at least 65 % of the brGDGTs in sediments from the Carminowe Creek in southwest England were produced in situ. Similarly, higher IR values in SPM than in catchment soils in the Madre de Dios River, an upper tributary of the Amazon River, could be linked with enhanced aquatic production in the dry season, when soil input into the river is limited (Kirkels et al., 2020a).

Upon discharge into the marine realm, the soil-derived brGDGT signal may be further altered by coastal marine brGDGT production. Such a marine contribution to the pool of brGDGTs can be identified using the weighted number of cyclopentane moieties in tetramethylated brGDGTs ($\#\text{rings}_{\text{tetra}}$), where values >0.7 indicate a purely marine origin (Sinninghe Damsté, 2016). As such, $\#\text{rings}_{\text{tetra}}$ has been used to reconstruct changes in the origin of brGDGTs over the Holocene in Baltic Sea sediments (Warden et al., 2018) and to correct for marine overprint on the terrestrial climate signal of soil-derived brGDGTs in Pliocene sediments from the North Sea basin (Dearing Crampton-Flood et al., 2018).

Isoprenoid GDGTs produced by archaea may provide independent information on OC sources in the river, as group I.1b Thaumarchaeota that thrive in soils produce more of the crenarchaeol isomer (cren′) compared to the aquatically produced group I.1a Thaumarchaeota (14 %–19 % and 0 %–3 % of all isoGDGTs, respectively; Pitcher et al., 2010, 2011; Kim et al 2012; Sinninghe Damsté et al., 2012; Elling et al., 2017; Bale et al., 2019). A high abundance of cren′ relative to that of crenarchaeol (defined as $f(\text{cren}')$) may thus indicate an input of soil material into the river. Furthermore, the ratio of GDGT-0 / crenarchaeol can be used to identify the presence of methanogens and other aquatic archaea that produce GDGT-0 in, for example, standing waters based on the finding that this ratio is <2 in cultured Thaumarchaeota (Blaga et al., 2009; Sinninghe Damsté et al., 2012).

In this study, we analyse a large set of soils, river SPM, and riverbed and estuarine sediments collected from the main stem and major tributaries of the Godavari River in peninsular India in a pre-monsoon (dry) and monsoon (wet) season to explore the evolution of GDGT distributions during transport along the land–river–sea continuum. The distinct wet and dry seasons in this river system allows us to investigate seasonal changes in the origin of GDGTs, i.e. soil-derived or aquatic-produced. In addition, different bedrock types in the upper and lower parts of the Godavari basin enable us to determine the provenance of the mineral fraction by looking at changes in the elemental composition of the riverbed sediments. Consequently, the mode of transport (free or mineral-associated) of the GDGTs can be assessed by direct comparison with the mineral elemental composition of the same soils and sediments (bulk and fine, i.e. $\leq 0.63\,\mu\text{m}$) they are extracted from. Possible influences by hydrodynamic sorting and/or selective transport of certain GDGTs are evaluated based on their occurrence and distribution along multiple depth profiles in the main stem Godavari and the delta. Finally, downcore variations in GDGT distributions in Holocene sediments from the Bay of Bengal give insight into the transfer efficiency of fluvially discharged GDGTs to the marine sedimentary archive and thus the reliability of GDGT-based paleorecords obtained from such archives.

2 Study area

The Godavari River is the largest monsoon-fed river of peninsular India. The Godavari has its source in the Western Ghats mountain range and flows eastward across central India before reaching the Bay of Bengal (Fig. 1). The Godavari has five major subbasins with a distinct hydrology and geology: the upper (~ 37 % of the total basin area), middle (6 %), and lower (2 %) Godavari cover the main stem of the river, whereas the north (35 %) and east tributaries (20 %) comprise contributions by the Wainganga, Penganga, Wardha, and Pranhita rivers and the Indravati and Sabari rivers, respectively (Babar and Kaplay, 2018) (Fig. 1b, c). We here refer to the upper Godavari and the north tributary headwaters (i.e. Wardha and Penganga rivers) that drain the Deccan Plateau as the upper basin and to all other north tributaries, east tributaries, and middle and lower Godavari as the lower basin.

The Godavari River has a catchment area of $3.1 \times 105\,\text{km}^2$, a length of 1465 km, and exports ~ 2.8 Mt of OC and 170 Mt of sediment to the Bay of Bengal annually (Biksham and Subramanian, 1988a, b; Gupta et al., 1997; Babar and Kaplay, 2018). Currently, a dam with a reservoir

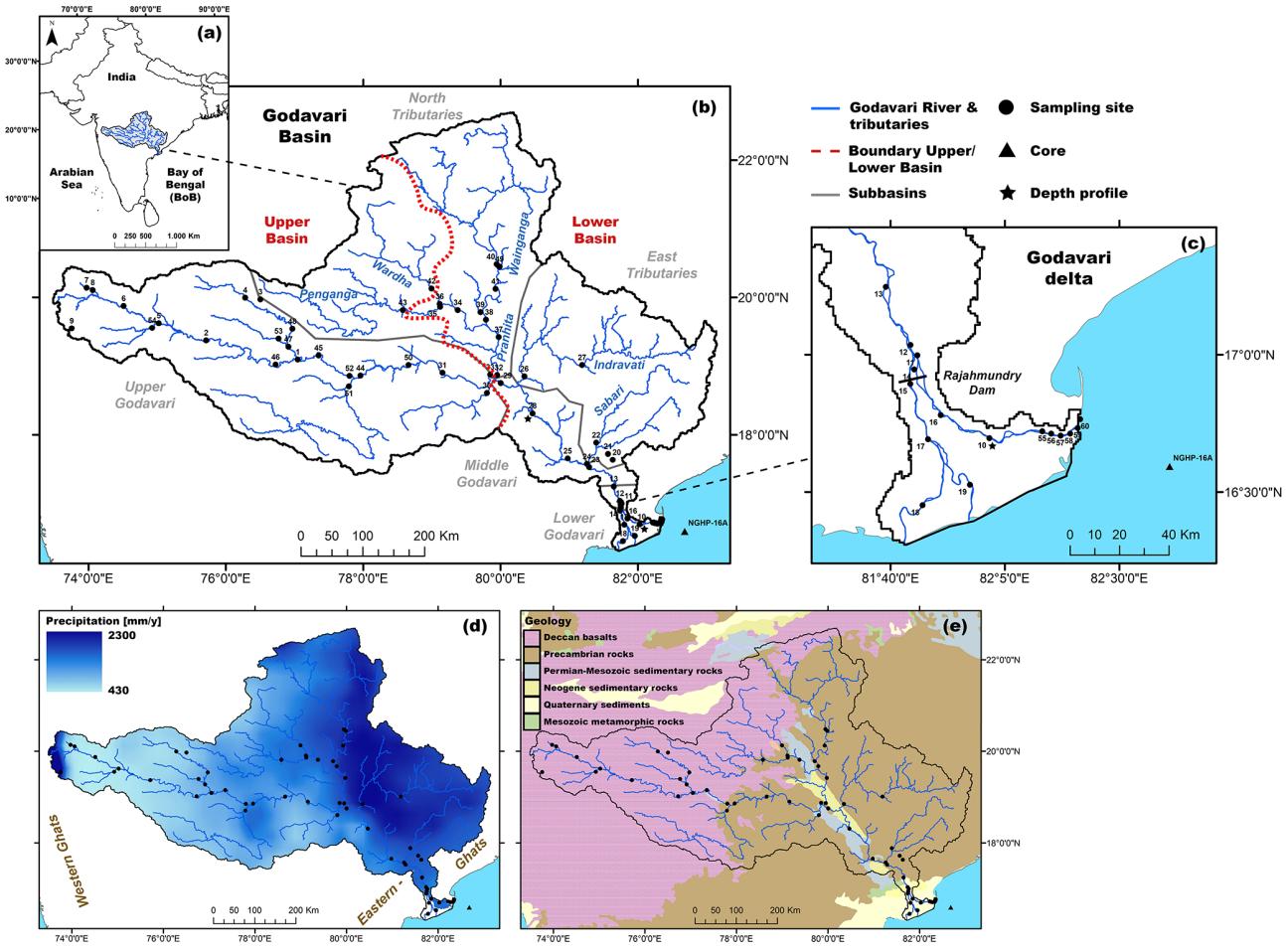

Figure 1. **(a)** Location of the Godavari River basin in peninsular India. **(b)** Sampling sites along the river basin, with the different subbasins (grey) and upper and lower basin (red) shown. **(c)** Zoom for the Godavari delta and the reservoir dam at Rajahmundry. **(d)** Precipitation across the Godavari basin based on the APHRODITE dataset (Asian Precipitation – Highly Resolved Observational Data Integration Towards Evaluation of Water Resources, V1101 Monsoon Asia) of mean annual precipitation for 30 years at a 0.25° grid resolution (Yatagai et al., 2012). **(e)** Geological context of the Godavari basin.

lake built in the mid-19th century at Rajahmundry controls the flow to the tidally influenced delta. In the delta, the river splits into three branches, of which the northern (Gautami) branch carries the majority (67 %) of the discharge and sediment load via an estuary to the Bay of Bengal (Rao et al., 2015). Smaller dams that control the river flow year-round are abundant in the upper basin (Pradhan et al., 2014).

The hydroclimate of the Godavari River basin is characterised by a distinct dry period (October–May) and a monsoon (wet) season (June–September). The southwest monsoon, with its main moisture source in the Indian Ocean and Arabian Sea, brings 75 %–85 % of the annual rainfall to the Godavari basin in the wet season (Balakrishna and Probst, 2005; Kirkels et al., 2020b). Approximately 94 % of the annual discharge and ∼ 98 % of the sediment load is exported during the monsoon (wet) season (Rao et al., 2015). The upper Godavari subbasin lies in the rain shadow of the Western Ghats mountain range and receives limited precipitation ($\sim 430\,\mathrm{mm\,yr^{-1}}$). The semi-arid climate of the upper basin gradually transitions to (sub-)humid conditions with increasingly more precipitation ($\sim 2300\,\mathrm{mm\,yr^{-1}}$) in the lower reaches (Gunnell, 1997; Babar and Kaplay, 2018) (Fig. 1d). Rainfall data from the year of sampling can be found in Kirkels et al. (2020b), and discharge data can be found in Fig. A1. The mean annual air temperature in the basin averages around 27 °C (Dearing Crampton-Flood et al., 2019a).

The headwaters of the upper Godavari (source to Nanded) and of the north tributaries (Wardha and Penganga rivers) drain the Deccan Plateau (Fig. 1e). This plateau consists of flood basalts of ∼ 200 to 2000 m thickness formed by volcanic activity across the Cretaceous–Tertiary boundary (65–66 Ma) that have weathered into thick, highly erodible clay loam layers (Biksham and Subramanian, 1988a, c; Keller et al., 2008; Meert et al., 2010), rich in iron oxides

and clay minerals (predominantly smectite) (Das and Krishnaswami, 2007; Babechuk et al., 2014; Usman et al., 2018). The lower stretches of the upper Godavari flow through (felsic) granite and gneiss complexes. The middle Godavari and the Pranhita and Wainganga rivers in the north subbasin drain Archean and Proterozoic (Precambrian) aged sedimentary and metamorphic rocks, Permian–Mesozoic Gondwana sediments which are mildly metamorphosed, mature shales, and (feldspathic) sandstones of Neogene age (Meert et al., 2010; Amarasinghe et al., 2015). This region is further characterised by active open-pit mining of near-surface coal deposits (Singh et al., 2012; Pradhan et al., 2014).

The east tributaries drain the Eastern Ghats mountains consisting of erosion-resistant, high-grade metamorphic rocks of Precambrian age, including khondalites (Si–Mg-rich), charnockites (quartz-feldspar), gneisses, and feldspar-rich granulites (Meert et al., 2010; Amarasinghe et al., 2015; Manikyamba et al., 2015). The lower Godavari River traverses thick layers of alluvium formed by Quaternary river deposits, underlain by Gondwana sandstones (Manikyamba et al., 2015). Source rock weathering in the lower reaches results in quartzo-feldspathic minerals and minor amounts of kaolinite (Usman et al., 2018). Soils range from 10–40 cm deep, clay-dominated, alkaline Vertisols interspersed with shallow Leptosols in the upper Godavari subbasin to deeper-developed, weathered, acidic Lixisols and Nitisols ("red soils") towards the east, as well as sandy Fluvisols and Arenosols towards the delta (Biksham and Subramanian, 1988b; WRB FAO, 2015; Giosan et al., 2017).

3 Materials and methods

3.1 River basin sampling

Surface soils (0–10 cm) were collected with a shovel from undisturbed sites near the Godavari River and its main tributaries during the dry season in February/March 2015 ($n = 46$), combining three to five spatial replicates (Fig. 1b, c). These topsoils represent material that may be eroded and transported into the river by the next precipitation events. Suspended particulate matter (SPM) was sampled during both dry (February/March 2015, $n = 50$) and wet seasons (July/August 2015, $n = 56$). At each sampling location, 20–80 L of surface water was collected at the mid-channel position by immersion of a bucket from a bridge or boat or otherwise from 2–3 m out of the riverbank. River depth profiles (two to three depths, one to three sites across the river) were sampled in the Godavari delta (main branch, dry and wet season) and in the main stem in the middle Godavari (wet season) (Fig. 1b, c; site 10 and 28). At these sites, river water was collected with equal increments to the riverbed as monitored by a mounted sonar instrument (Humminbird PiranhaMAX 153), using a custom-built depth sampler (after Lupker et al., 2011). After collection, the river water was transferred into pre-rinsed containers and filtered over pre-combusted (450 °C, 6 h) and pre-weighted 0.7 µm glass fibre filters (GFFs) (Whatman, United Kingdom) using pressurised steel filtration units (after Galy et al., 2007) to obtain the SPM. Riverbed sediments were collected at the mid-channel position during both dry ($n = 37$) and wet ($n = 37$) seasons, using an Eijkelkamp sediment grabber (Van Veen grab 04.30.01, the Netherlands) or a shovel when the water level was low. At selected sites, soils ($n = 10$) and wet-season riverbed sediments ($n = 25$) were sieved in the field to isolate the fine fraction ≤ 63 µm.

All SPM filters were kept at 4 °C and soils and sediments at ambient temperature after collection and subsequent transport to the laboratory at Utrecht University, where all materials were stored frozen (−20 °C) and then freeze-dried. SPM filters were weighted to determine sediment loads. Bulk soils and riverbed sediments were homogenised by manual removal of stones and plant debris and then ground to a fine powder using a stainless-steel/agate mortar or ball mill (OC and biomarker analysis) or a Herzog mill (elemental analysis). Sampling procedures for the marine sediment core NGHP-01-16A (16.59331° N, 82.68345° E; 1268 m water depth; $n = 46$) in the Bay of Bengal are described in Ponton et al. (2012) and Usman et al. (2018).

3.2 pH measurements

River water pH was measured in the field with an HQ40d multi-parameter meter (Hach, USA), fitted with a pH probe (IntelliCAL PHC101). The pH of bulk soils and riverbed sediments was measured upon return to the laboratory, using a SympHony SB70D with a pH probe (VWR, USA) and distilled water to create a 1 : 5 (v/v) solid to water mixture after shaking for 30 min at 200 rpm and settling overnight ($\sim$ 18 h at 4 °C).

3.3 Total organic carbon analysis

The total organic carbon (TOC) content of bulk soil, bulk riverbed sediments, and SPM was analysed with a Flash 2000 organic element analyser equipped with a MAS 200 autosampler (Thermo Scientific, Italy) at NIOZ (Texel, the Netherlands). Prior to analysis, powdered riverbed and soil samples were decalcified by adding 1M HCL, mixed, and subsequently rinsed 2 times with distilled water and dried at 60 °C. For SPM, pieces of GFFs were randomly selected and placed in pre-combusted (450 °C, 6 h) Ag capsules. These capsules were put in a desiccator at 70 °C with 37 % HCl for 72 h (decalcification) and subsequently dried for minimal 120 h with NaOH (neutralisation) (Komada et al. 2008; van der Voort et al., 2016). Fine-fraction (≤ 63 µm) riverbed sediments and soils were analysed with a NC2500 elemental analyser (ThermoQuest, Germany) at Vrije Universiteit Amsterdam (the Netherlands). These fine fractions were placed in pre-combusted Ag cups and acidified in situ by adding 1M

HCl and subsequently dried overnight at 60 °C (Vonk et al., 2008, 2010). TOC results were normalised to internal standards (acetanilide and benzoic acid at NIOZ and USGS40, USGS41, and IAEA601 at Vrije Universiteit Amsterdam), with an analytical reproducibility better than 0.07 % based on replicate analysis of standards and samples.

3.4 Soil and sediment elemental composition

Major and trace elements were measured by inductively coupled plasma optical emission spectrometry (ICP-OES) using a Spectro Arcos (Ametek, Germany) at Utrecht University for soils and riverbed sediments (bulk and fine fractions). Approximately 100–125 mg of freeze-dried and powdered soil or sediment was digested in a 2.5 mL acid mixture ($HClO_4 : HNO_3$; 3 : 2 (v/v)) with 2.5 mL 48 % HF and heated at 90 °C overnight. Next, the acid mixture was evaporated at 140 °C, and the residue was dissolved overnight in 1M HNO_3 at 90 °C for elemental analysis. Replicate analyses of selected samples gave a precision of ± 3 % for the major elements and ± 10 % for titanium.

3.5 GDGT extraction and analysis

All bulk and fine-fraction soils and riverbed sediments were analysed for GDGTs. For SPM, a selection was made for the dry ($n = 20$) and wet seasons ($n = 49$). The freeze-dried and powdered soils (∼ 2–20 g), riverbed sediments (∼ 1–18 g), and SPM (∼ 0.04–5 g on filter pieces) were extracted with dichloromethane (DCM) : methanol (MeOH) (9 : 1, v/v) using an accelerated solvent extractor (ASE 350, Dionex) at 100 °C and 7.6 × 106 Pa. The total lipid extracts (TLEs) were dried under a gentle stream of N_2. TLEs of wet-season SPM and bulk soils were saponified with KOH in MeOH (0.5 M, 2 h at 70 °C). Separation was enhanced by adding distilled water with NaCl, after which the neutral fraction was back-extracted with hexane (3 × 10 mL). The remaining mixture was acidified to pH ∼ 2 by adding 1.5 M HCl (dissolved in MeOH) and back-extracted (3 × 10 mL) with hexane : DCM (4 : 1, v/v) to isolate the acid fraction containing fatty acids for further use by Usman et al. (2018). For our study, the neutral fraction was passed over a Na_2SO_4 column to remove water and further separated over an activated Al_2O_3 column into an apolar and polar fraction using hexane and DCM : MeOH (1 : 1, v/v) as eluents, respectively. TLEs of dry-season SPM, riverbed sediments (bulk and fine fraction ≤ 63µm), and fine-fraction soils were directly fractionated into an apolar, neutral, and polar fraction by passing over an activated Al_2O_3 column using hexane, hexane : DCM (1 : 1, v/v), and DCM : MeOH (1 : 1, v/v) as eluents, respectively. Due to the ambient temperatures at which soils and riverbed sediments were stored during our field campaign and transport to the lab at Utrecht University, the use of an ASE that uses high temperature and pressure, and the fact that mineral soils contain relatively minor amounts of intact polar lipid (IPL) GDGTs (e.g. Peterse et al., 2010; Huguet et al., 2010; Zell et al., 2013b), we have assumed that the slightly different workup procedures will have no impact on the concentrations and relative abundances of the GDGTs in this study.

All polar fractions containing the GDGTs were spiked with a C_{46} GTGT as internal standard (Huguet et al., 2006), dried, re-dissolved in hexane : isopropanol (99 : 1, v/v), and passed over a 0.45 µm polytetrafluoroethylene (PTFE) filter prior to analysis. GDGTs were measured using ultra-high-performance-liquid-chromatography atmospheric-pressure-chemical-ionisation mass spectrometry (UHPLC-APCI-MS) with an Agilent 1260 Infinity coupled to an Agilent 6130 quadrupole mass detector (Agilent Technologies, USA) at Utrecht University with settings according to Hopmans et al. (2016).

In brief, GDGTs were separated over two silica Waters Acquity UPLC BEH HILIC columns (150 × 2.1 mm; 1.7 µm; Waters corp., USA) maintained at 30 °C and preceded by a guard column packed with the same material. The compounds eluted isocratically with 82 % A and 18 % B for 25 min at 0.2 mL min^{-1}, followed by a linear gradient to 70 % A and 30 % B for 25 min and then to 100 % B in 30 min, where A is hexane and B is hexane : isopropanol (9 : 1, v/v). Sample injection volume was 10 µL. APCI settings were as follows: gas temperature, 200 °C; vaporiser temperature, 400 °C; drying gas (N_2) flow, 6 L min^{-1}; capillary voltage, 3500 V; nebuliser pressure, 60 psi; corona current, 5.0 µA. Detection was achieved in selected ion monitoring mode (SIM), using m/z 744 for the standard; m/z 1302, 1300, 1298, 1296, and 1292 for isoGDGTs; and m/z 1050, 1048, 1046, 1036, 1034, 1032, 1022, 1020, and 1018 for brGDGTs.

Core samples (NGHP-01-16A) were extracted by Usman et al. (2018), and the polar fractions were analysed for only brGDGTs at NIOZ (the Netherlands) using the same UHPLC method and settings. The same core was extracted previously by Ponton et al. (2012) at a lower resolution and analysed for both isoprenoid and branched GDGTs at ETH Zürich (Switzerland) using a Grace Prevail Cyano column (150 × 2.1 mm; 3 µm) and settings according to Schouten et al. (2007) that do not separate 5- and 6-methyl brGDGTs. Agilent ChemStation software (B.04.03) was used to integrate peak areas in the mass chromatograms of the protonated molecule ($[M+H]^+$).

3.6 Proxy calculations

GDGT indices were calculated using the fractional abundances of specific GDGTs. Roman numerals in all formulas refer to the molecular structures of brGDGTs shown in De Jonge et al. (2014a) and of isoGDGTs in Kim et al. (2010). Spatial and temporal variations in GDGT signals were assessed using the degree of cyclisation of branched tetraethers,

calculated according to De Jonge et al. (2014a),

$$\mathrm{CBT}' = {}^{10}\log\left(\left(\mathrm{Ic}+\mathrm{IIa}'+\mathrm{IIb}'+\mathrm{IIc}'+\mathrm{IIIa}'+\mathrm{IIIb}'+\mathrm{IIIc}'\right) / \left(\mathrm{Ia}+\mathrm{IIa}+\mathrm{IIIa}\right)\right), \quad (1)$$

as well as the degree of methylation of 5-methyl brGDGTs,

$$\mathrm{MBT}'_{5\mathrm{Me}} = \left(\mathrm{Ia}+\mathrm{Ib}+\mathrm{Ic}\right) / \left(\mathrm{Ia}+\mathrm{Ib}+\mathrm{Ic}+\mathrm{IIa}+\mathrm{IIb}+\mathrm{IIc}+\mathrm{IIIa}\right). \quad (2)$$

Translation of brGDGT distributions into mean annual air temperatures (MAATs) was done using the $\mathrm{MBT}'_{5\mathrm{Me}}$ index and the BayMBT_0 model (MATLAB R2020a, v.9.8.0.1323502), following Dearing Crampton-Flood et al. (2020). A prior mean of 27.2 °C, which is the average measured MAAT for the Godavari basin extracted from the 0.5° gridded climatic research unit gridded time series (CRU TS) v. 3.24.01 dataset (Dearing Crampton-Flood et al., 2020), and a prior standard deviation of 10 °C were chosen as model input.

Potential in situ production of brGDGTs within the river was assessed using the isomer ratio (IR) of pentamethylated and hexamethylated brGDGTs (Dang et al., 2016, modified from De Jonge et al., 2014b):

$$\mathrm{IR} = \left(\mathrm{IIa}'+\mathrm{IIb}'+\mathrm{IIc}'+\mathrm{IIIa}'+\mathrm{IIIb}'+\mathrm{IIIc}'\right) / \left(\mathrm{IIa}+\mathrm{IIb}+\mathrm{IIc}+\mathrm{IIIa}+\mathrm{IIIb}+\mathrm{IIIc}+\mathrm{IIa}'+\mathrm{IIb}'+\mathrm{IIc}'+\mathrm{IIIa}'+\mathrm{IIIb}'+\mathrm{IIIc}'\right). \quad (3)$$

To identify contributions of marine in situ production of brGDGTs, the weighted average number of cyclopentane moieties of the tetramethylated brGDGTs was calculated following Sinninghe Damsté (2016),

$$\#\mathrm{rings}_{\mathrm{tetra}} = \left(\mathrm{Ib}+2\times\mathrm{Ic}\right) / \left(\mathrm{Ia}+\mathrm{Ib}+\mathrm{Ic}\right), \quad (4)$$

as well as the ratio of acyclic hexamethylated to pentamethylated brGDGTs, including 6-methyl brGDGTs (Xiao et al., 2016, 2020),

$$\Sigma\mathrm{IIIa}/\Sigma\mathrm{IIa} = \left(\mathrm{IIIa}+\mathrm{IIIa}'\right) / \left(\mathrm{IIa}+\mathrm{IIa}'\right). \quad (5)$$

The branched and isoprenoid tetraether (BIT) index was calculated following Hopmans et al. (2004), adjusted to include 6-methyl brGDGTs:

$$\mathrm{BIT\ index} = \left(\mathrm{Ia}+\mathrm{IIa}+\mathrm{IIa}'+\mathrm{IIIa}+\mathrm{IIIa}'\right) / \left(\mathrm{Ia}+\mathrm{IIa}+\mathrm{IIa}'+\mathrm{IIIa}+\mathrm{IIIa}'+\mathrm{crenarchaeol}\right). \quad (6)$$

The relative contribution of the crenarchaeol isomer was calculated using

$$f\left(\mathrm{cren}'\right) = \left(\mathrm{cren}'\right) / \left(\left(\mathrm{cren}'+\mathrm{crenarchaeol}\right)\right). \quad (7)$$

Sea surface temperatures (SSTs) were estimated based on isoGDGTs extracted from the NGHP-01-16A core by Ponton et al. (2012) and the relation between TEX_{86}^{H} and SST derived by Kim et al. (2010):

$$\mathrm{TEX}_{86}^{\mathrm{H}} = \log\left(\left(\mathrm{GDGT}-2+\mathrm{GDGT}-3+\mathrm{cren}'\right) / \left(\mathrm{GDGT}-1+\mathrm{GDGT}-2+\mathrm{GDGT}-3+\mathrm{cren}'\right)\right), \quad (8)$$

$$\mathrm{SST} = 68.4\times\mathrm{TEX}_{86}^{\mathrm{H}} + 38.6. \quad (9)$$

3.7 Statistical analysis

The significance of differences in brGDGT concentrations, distributions, and proxy values for each sample type, season, or location in the basin was evaluated with (Welch's) ANOVA and t tests in the R software package for statistical computing (RStudio, v. 1.2.5033; R4.0.4) and SPSS (IBM, v. 26.0.0.0). The level of significance was $p \leq 0.05$. Results are reported as mean ± standard error (SE). Spatial patterns were further investigated with ArcGIS 10.6.1 software (ESRI, USA). Principal component analysis (PCA) was performed in the R package FactoMineR (Lê et al., 2008) using the relative abundances of the most abundant brGDGTs (i.e. Ia, Ib, Ic, IIa, IIa′, IIb′, IIIa, and IIIa′). Linear correlations were assessed by Pearson correlation coefficients.

4 Results

4.1 Physical and chemical properties of Godavari River water, SPM, sediments, and soils

4.1.1 Suspended sediment load

All geochemical data can be found in Kirkels et al. (2021a). Suspended sediment loads in surface waters of the Godavari ranged from 1 to 135 mg L^{-1} in the dry season (14 ± 4 mg L^{-1} (mean ± SE), $n=41$) and from 2 to 1435 mg L^{-1} in the wet season (149 ± 37 mg L^{-1}, $n=40$) (Fig. 2a). Average suspended loads were significantly higher in the wet season ($p \leq 0.001$), with concentrations up to 75 to 170 times higher at certain sites compared to the dry season, especially in the Pranhita River (north tributaries) and the middle and lower Godavari. In contrast, the upper Godavari and those north tributaries that drain the Deccan Plateau had low suspended loads (mostly < 50 mg L^{-1}). In the dry season, spatial variability in sediment load was minor. The depth profiles taken in the main stem Godavari and the delta (site 28 and 10, respectively; Fig. 1b, c) show that suspended sediment concentrations did not substantially vary with depth in both the dry and wet season (Fig. 3a). A slight increase in suspended load above the riverbed was only observed at the site closest to the eroding riverbank in the Godavari delta (Fig. 3a).

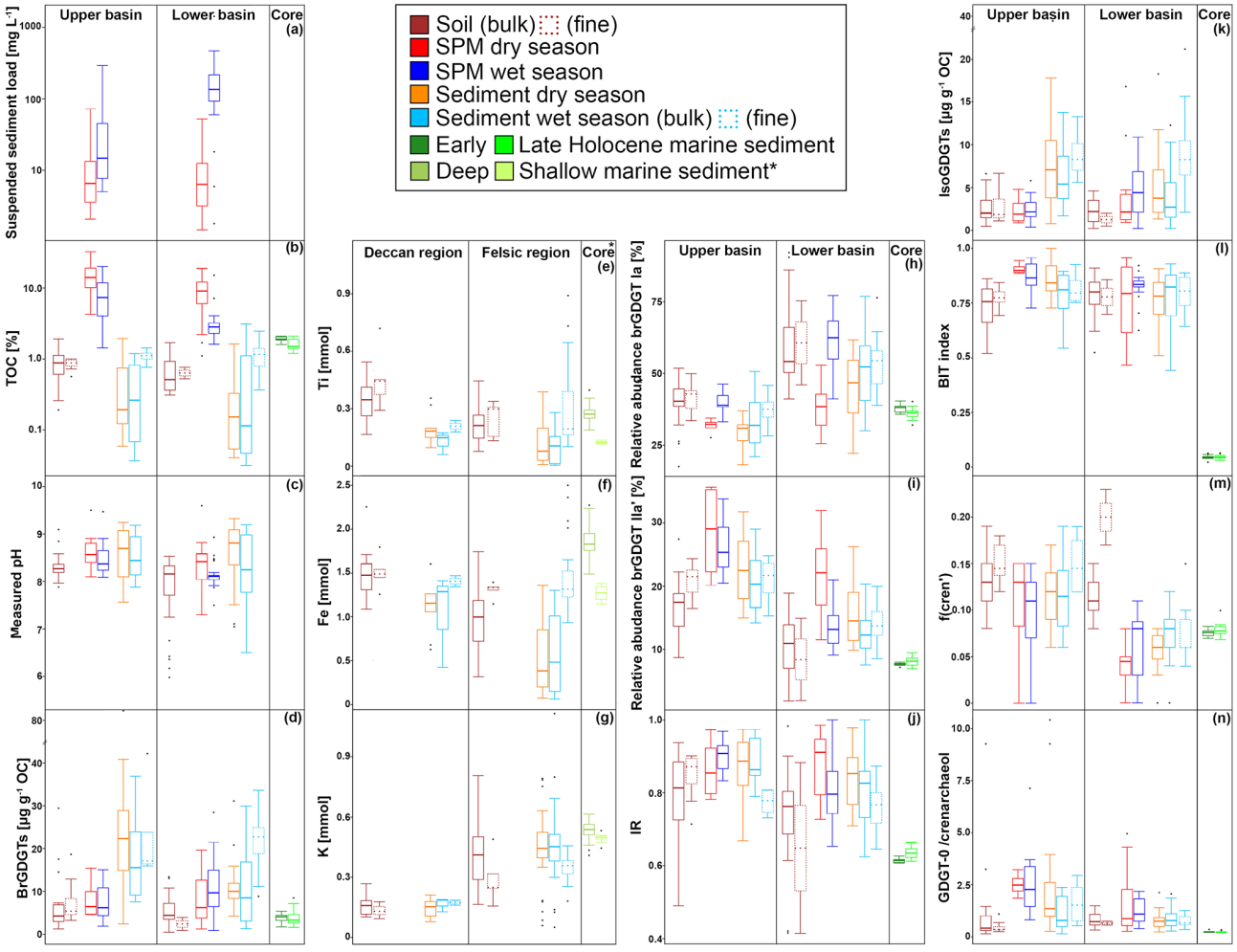

Figure 2. Box-and-whisker plots of the organic, geochemical, and GDGT data for the Godavari basin and marine sediments in the Bay of Bengal. **(a)** Suspended sediment load, **(b)** total organic carbon (TOC), **(c)** measured pH, and **(d)** brGDGT concentrations normalised to % OC in the upper and lower basin and in Holocene marine sediments. **(e)** Ti, **(f)** Fe, and **(g)** K amounts in the Deccan basalt and felsic bedrock regions, and * in shallow (0–48 cm b.s.f., ∼ 300 years; Kalesha et al., 1980) and deep marine sediments (0–300 m (NGHP-1-3B) and 0–184 m b.s.f. (NGHP-1-5C), no age model used; Mazumdar et al., 2015). **(h)** Relative abundance of brGDGT Ia, **(i)** relative abundance of brGDGT IIa′, and **(j)** isomer ratio (IR) values in the upper and lower basin and in Holocene marine sediments. **(k)** Isoprenoid GDGT concentrations normalised to % OC, **(l)** BIT index, **(m)** f(cren′), and **(n)** GDGT-0 / crenarchaeol in the upper and lower basin and in Holocene marine sediments. The box represents the first (Q1) and third (Q3) quartiles, and the line in the box represents the median value; the whiskers extend to 1.5 × (Q3–Q1) values, and outliers are shown as points. Solid lines represent bulk data, and dashed lines represent the fine fractions (≤ 63 µm). The pH represents values measured in soil and sediment extracts and in surface water for SPM.

4.1.2 Total organic carbon

The organic carbon content (% OC) in soils was between 0.2 % and 1.9 % (0.8 ± 0.1, $n = 46$) for the bulk and between 0.5 % and 1.0 % (0.8 ± 0.1 %, $n = 10$) for the fine fractions (Fig. 2b). The % OC was generally higher in fine-fraction soils than in bulk soils from the same site (0.82 ± 0.05 % vs. 0.69 ± 0.07 %, $p = 0.06$, $n = 10$). There was no spatial trend in % OC in soils across the basin.

The % OC in surface SPM collected during the dry season varied between 1.1 % and 32.4 % (11.4 ± 1.1 %, $n = 39$) and was significantly higher than that in wet-season SPM (1.4 %–20.1 %, 5.2 ± 0.7, $n = 40$, $p \leq 0.001$). In both seasons, the % OC of surface SPM from the upper basin was significantly higher than that from the lower basin (dry: 15.5 ± 2.2 %, $n = 13$, vs. 9.4 ± 1.0 %, $n = 26$, $p \leq 0.01$; wet: 8.4 ± 1.5 %, $n = 14$, vs. 3.5 ± 0.5%, $n = 26$, $p \leq 0.01$). In the dry season, the % OC of surface SPM decreased downstream, changing from 15.2 ± 2.3 % ($n = 11$) in the upper Godavari, 12.4 ± 2.1% ($n = 10$) in the north, and 7.6 ± 1.1 % ($n = 6$) in the east tributaries to 13.3 ± 2.8 % ($n = 4$) and 7.0 ± 1.9 % ($n = 8$) in the middle and lower Godavari, respectively. In the wet season, the % OC of SPM showed a stronger decrease downstream ($p \leq 0.05$) and changed from

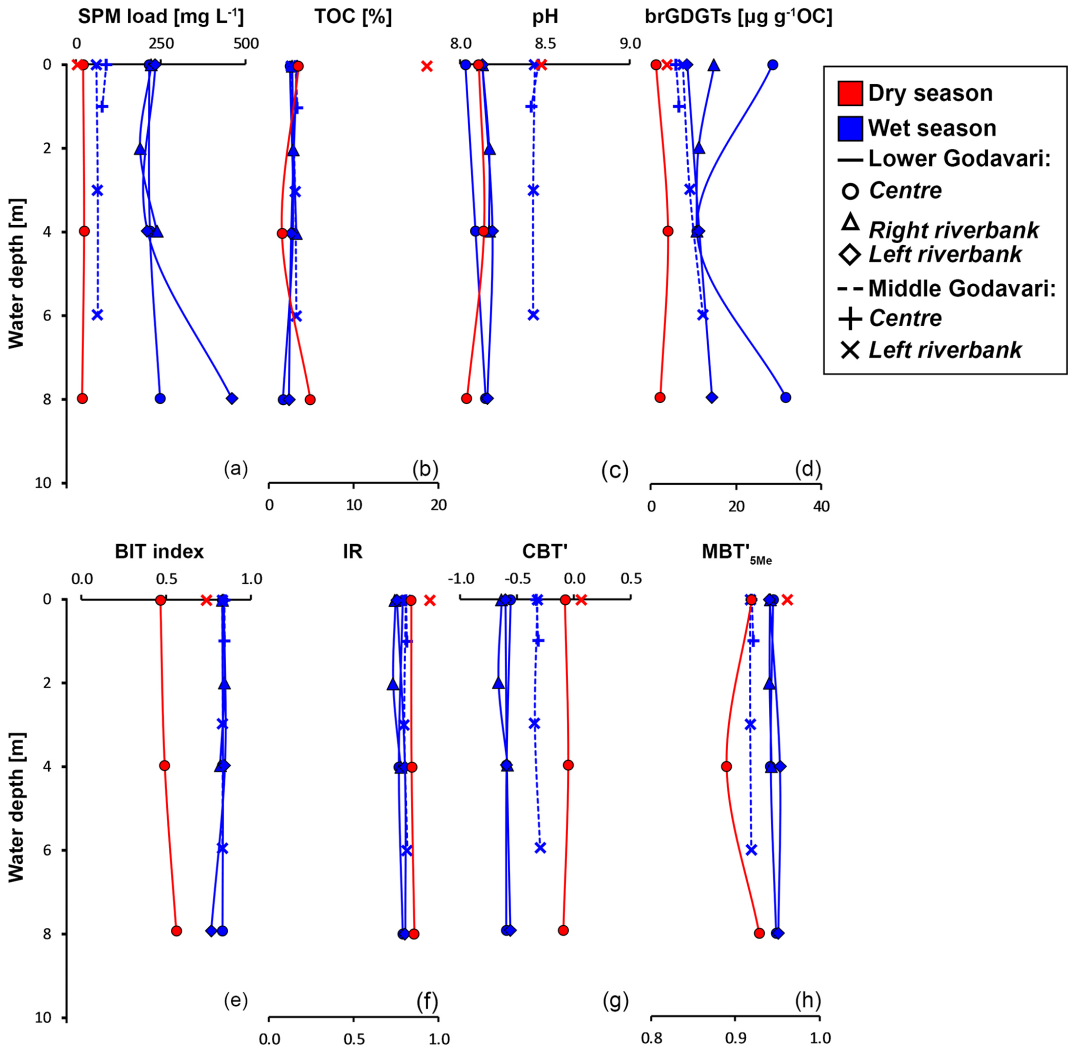

Figure 3. River depth profiles of bulk properties: **(a)** suspended particulate matter (SPM) load, **(b)** total organic carbon (TOC), **(c)** measured pH in the water column, and **(d)** brGDGT concentration. River depth profiles of brGDGT-based indices: **(e)** BIT index, **(f)** isomer ratio (IR), **(g)** CBT′, and **(h)** MBT'_{5Me} index values. The symbols represent the position in the channel: mid-channel (centre) and near the left and right riverbank. In the lower Godavari, the right is the non-eroding riverbank and the left is the eroding riverbank.

9.2 ± 1.6 % ($n = 12$) in the upper Godavari, 2.5 ± 0.2 % ($n = 9$) in the north, and 6.6 ± 3.1 % ($n = 4$) in the east tributaries to 4.0 ± 0.8 % ($n = 5$) in the middle and 2.8 ± 0.2 % ($n = 10$) in the lower Godavari. The % OC in SPM showed minor variation (<1 % and mostly <0.54 %) along the depth profiles collected in both the dry and wet season (Fig. 3b).

Bulk riverbed sediments had on average a lower % OC in the dry season (0.4 ± 0.1 %, 0.04 %–19.5 %, $n = 37$) than in the wet season (0.6 ± 0.1 %, 0.03 %–3.1 %, $n = 37$). The riverbed sediments showed no spatial trend in % OC across the Godavari basin in either season. Fine fractions collected in the wet season had a significantly higher % OC than the bulk riverbed sediments at the same sites (fine: 1.2 ± 0.1 %, bulk: 0.7 ± 0.2 %, $n = 25$, $p \leq 0.01$).

4.1.3 Measured pH

The pH measured in soils in the Godavari basin ranged from 6.0 to 9.1 ($n = 46$), with generally higher pH (mostly >8.0) in the soils from the upper basin and lower pH (mostly <8.0) in the lower basin (Fig. 2c). The in situ-measured pH of surface waters and the pH of riverbed sediments were on average slightly higher in the dry season (water: 8.4 ± 0.1, $n = 46$; sediment: 8.6 ± 0.1, $n = 37$) than in the wet season (water: 8.2 ± 0.0, $n = 47$, $p \leq 0.03$; sediment: 8.3 ± 0.1, $n = 37$, $p \leq 0.09$). In both seasons, river water pH was relatively constant with river depth (Fig. 3c).

4.1.4 Soil and sediment elemental composition

The elemental composition of soils and sediments is different between (i) those parts of the upper Godavari and north tributary headwaters that drain the Deccan basalts and (ii) the lower reaches of the Godavari basin that drain felsic metamorphic and sedimentary rocks (Fig. 2e–g). In particular, Ti and Fe concentrations in bulk soils from the Deccan basalts were significantly higher than those formed on felsic rocks in the lower part of the basin (Ti: 0.34 ± 0.03, $n = 13$, vs. 0.21 ± 0.02 mmol, $n = 34$, $p \leq 0.001$; Fe: 1.50 ± 0.08 vs. 0.97 ± 0.06 mmol, $p \leq 0.001$). In contrast, K concentrations were significantly lower in Deccan soils than those formed on felsic rocks (0.16 ± 0.01 vs. 0.41 ± 0.03 mmol, $p \leq 0.001$). Riverbed sediments showed the same spatial division in these elements, although less pronounced for Ti and Fe in the wet season. Comparison of bulk and fine-fraction soils revealed no differences ($p \geq 0.05$), whereas fine-fraction sediments in the wet season contained more Ti and Fe and less K compared to the bulk sediments ($p \leq 0.01$).

4.2 Concentrations and distribution of GDGTs in soils, SPM, riverbed sediments of the Godavari River, and downcore Bay of Bengal sediments

4.2.1 GDGTs in catchment soils

The soils analysed in this study ($n = 46$) were previously included in a global dataset to develop a Bayesian calibration model (Dearing Crampton-Flood et al., 2019a, 2020), but brGDGT concentrations and distributions have not yet been described in detail. In short, brGDGTs were detected in all Godavari soils and ranged in concentration from 0.4 to 29.5 $\mu g\,g^{-1}$ OC ($5.9 \pm 0.8\,\mu g\,g^{-1}$ OC), without a clear spatial trend across the basin (Fig. 2d). Branched GDGT concentrations in fine fractions averaged $6.5 \pm 1.7\,\mu g\,g^{-1}$ OC (0.8–18.7, $n = 10$), and they are comparable to that in the bulk soil at the same site. Branched GDGT Ia was the most abundant compound (18 %–92 %, 50 ± 2 %) contributing to >50 % of the brGDGTs in soils along the Pranhita River (north tributary), along the east tributaries, and downstream along the middle and lower Godavari subbasins ($n = 25$) (Fig. 4a). In contrast, the relative abundance of brGDGT Ia was <50 % in soils from the upper basin ($n = 21$, $p \leq 0.001$), where brGDGT Ib was the most dominant compound at a few sites instead (28 %–53 %, $n = 3$, sites 42, 46, 54; Figs. 2h, 4b). Contributions of brGDGTs IIb, IIc, IIc′, IIIb, IIIb′, IIIc, IIIc′, and IIIa rarely exceeded 2 %, and also IIIa′ contributed mostly ≤ 2 %. The fine fractions had similar brGDGT distributions as bulk soils ($p > 0.05$), albeit with slightly higher relative abundances of IIa′ (18 ± 2 %) at the expense of Ia (Figs. 2h, 4a, b). The relative contribution of 6-methylated isomers to brGDGTs in bulk soils varied spatially ($p \leq 0.001$) and were highest in the upper Godavari (26 ± 1 %, $n = 19$) and lowest in the east tributaries (6 ± 2 %, $n = 6$).

The concentration of isoGDGTs in bulk soils ranged from 0.2 to 6.6 $\mu g\,g^{-1}$ OC (2.5 ± 0.2) (Fig. 2k), of which crenarchaeol was the most abundant isoGDGT in most of the soils ($n = 33$) (Kirkels et al., 2022). This results in BIT index values of 0.52 to 0.91 (0.75 ± 0.01), where the lowest values (<0.65) occurred in the upper Godavari subbasin and in disturbed soils (i.e. agricultural soils or soils influenced by mining activities) from the north tributaries and lower Godavari (Fig. 2l). The $f(\text{cren}')$ ranged between 0.08 and 0.19 without a clear spatial pattern (Fig. 2m). The ratio of GDGT-0 / crenarchaeol varied between 0.2–9.3, where the highest values occurred in soils from the upper basin, although average values for the upper and lower basin are not significantly different ($p < 0.001$) (Fig. 2n). The fine fractions ($n = 10$) had similar concentrations, $f(\text{cren}')$, and GDGT-0 / crenarchaeol values to the bulk soils.

4.2.2 GDGTs in surface SPM

Branched GDGTs were detected in all SPM samples, but brGDGT IIIc was always below the detection limit. Branched GDGTs IIc, IIIa, IIIb, IIIb′, and IIIc′ had relative abundances ≤ 0.01, and contributions of brGDGTs IIb and IIc′ rarely exceeded 2 % in both the dry and wet season (Fig. 4a). In surface SPM collected in the dry season ($n = 18$), brGDGT concentrations were between 1.2 and 19.6 $\mu g\,g^{-1}$ OC (average 8.1 ± 1.2), without a distinct trend across the basin (Fig. 2d). Branched GDGT Ia generally dominated in SPM from the lower Godavari, whereas brGDGT IIa′ was the most abundant compound in the upper Godavari and north tributaries (Figs. 2h, i, 4c). The contribution of 6-methyl brGDGTs ranged from 20 % to 60 % (41 ± 3 %), with slightly higher contributions in the upper basin (47 ± 6 %, $n = 4$) than in the lower basin (39 ± 3 %, $n = 14$). Isoprenoid GDGTs were also present in all SPM samples, although cren′ was below the detection limit in three samples, and in four samples only GDGT-0 and crenarchaeol could be detected. Isoprenoid GDGT concentrations varied from 0.9 to 16.8 $\mu g\,g^{-1}$ OC (3.6 ± 1.0, $n = 18$) (Fig. 2k), of which GDGT-0 was the most abundant compound in the majority of the samples ($n = 10$), followed by crenarchaeol, resulting in BIT values between 0.47 and 0.96 (0.79 ± 0.04). The BIT was significantly higher in the upper basin (0.91 ± 0.01, $n = 4$) than in the lower basin (0.76 ± 0.05, $n = 14$, $p \leq 0.01$) (Fig. 2l) and decreased downstream to ≤ 0.75 in the middle and lower Godavari. The $f(\text{cren}')$ ranged from 0.03–0.15 and was higher in the upper basin (0.10 ± 0.04, $n = 4$) than in the lower basin (0.04 ± 0.01, $n = 14$) (Fig. 2m). The ratio of GDGT-0 / crenarchaeol varied from 0.3–5.0, where values were always >2 in the upper basin, as well as for sites with reduced flow in the lower basin (Fig. 2n).

Branched GDGT concentrations in surface SPM collected in the wet season ($n = 40$) varied between 0.8 and

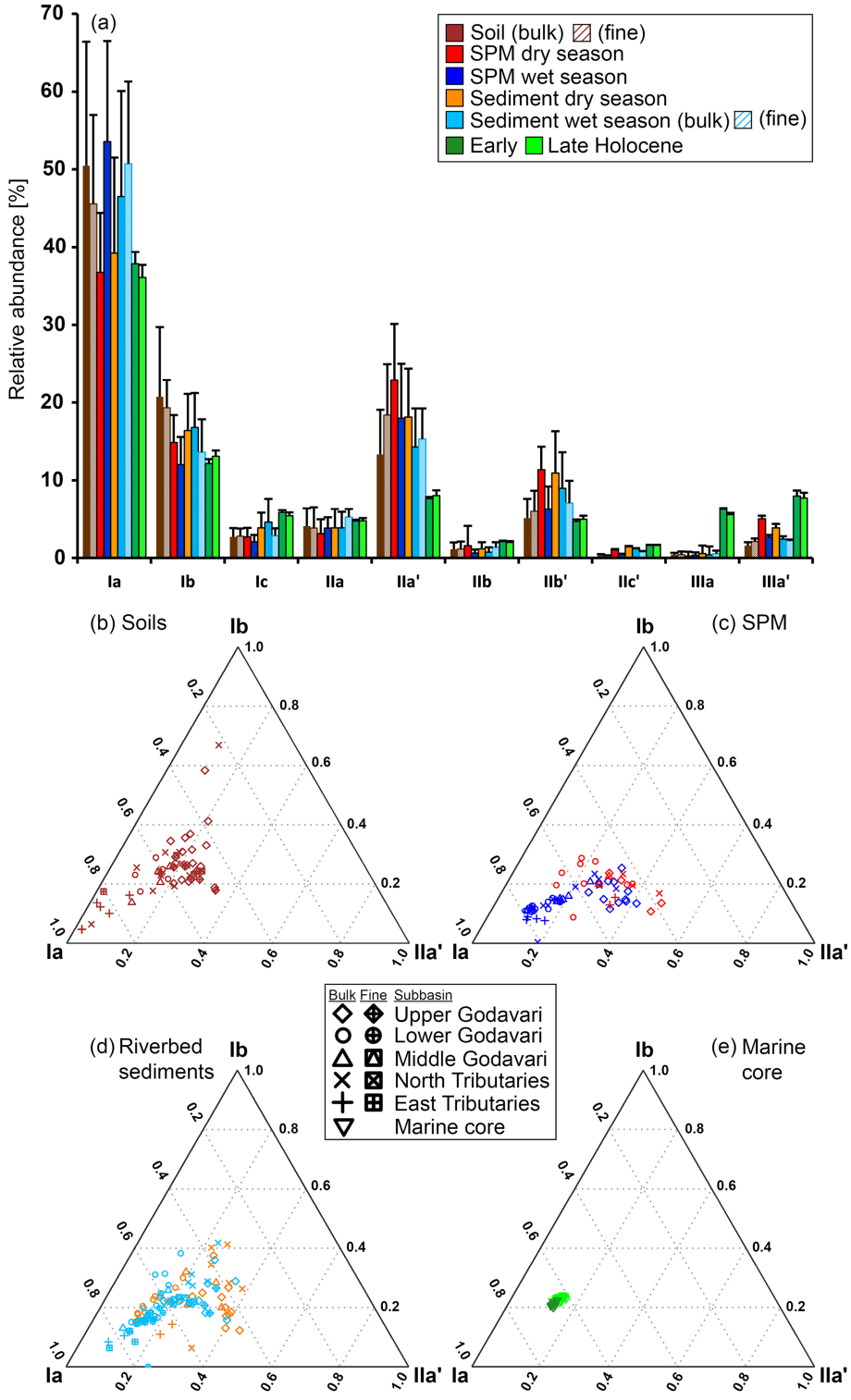

Figure 4. Branched GDGT distributions in the Godavari basin and in marine sediments from the Bay of Bengal. **(a)** Average relative abundances of brGDGTs in soils, SPM, and riverbed sediments in the dry and wet season, as well as in Holocene marine sediments. The error bars represent the standard deviation. The fine-fraction soils and sediments ($\leq 63\,\mu m$) are striped. Proportions of major brGDGTs Ia, IIa′, and Ib in **(b)** soils, **(c)** SPM, and **(d)** riverbed sediments and in a **(e)** Holocene marine core. The symbols represent the different subbasins, with open symbols for the bulk soils and sediments and enclosed symbols for the fine fractions.

$28.5\,\mu g\,g^{-1}$ OC (9.7 ± 1.0) (Fig. 2d) and showed no clear spatial variability. The OC-normalised brGDGT concentrations were similar to that in SPM in the dry season but almost ~ 2 times higher than in Godavari soils (Fig. 2d). In contrast to their concentration, brGDGT distributions did vary spatially. For example, the average contribution of brGDGT Ia was significantly lower in the upper basin than in the lower basin (40 ± 1 % vs. 61 ± 2 %, $p \leq 0.001$) (Fig. 2h), whereas brGDGT IIa′ showed an opposite trend from 26 ± 1 % in the upper basin to 14 ± 1 % in the lower basin ($p \leq 0.001$) (Fig. 2i). Similarly, the contribution of 6-methyl isomers was significantly higher in the upper basin (40 ± 1 %, $n = 14$) than in the lower basin (21 ± 1 %, $n = 26$; $p \leq 0.001$), following the trend in Godavari soils. The average contribution of 6-methyl brGDGTs in wet-season SPM was 28 ± 2 %, which is lower than in the dry season. Isoprenoid GDGT concentrations varied from 0.2 to $10.9\,\mu g\,g^{-1}$ OC (3.9 ± 0.5), of which GDGT-0 was the major compound in 22 samples, followed by crenarchaeol, resulting in BIT values between 0.62 and 0.96 (0.84 ± 0.01) (Fig. 2k, l). The BIT was significantly higher in the upper basin (0.87 ± 0.02) than in the lower basin (0.83 ± 0.01, $p \leq 0.05$) (Fig. 2l), similar to dry-season SPM. The $f(\text{cren}')$ and GDGT-0 / crenarchaeol varied in the same ranges as in the dry season, where the highest values occurred for SPM from the upper basin (Fig. 2m, n).

4.2.3 GDGTs in SPM depth profiles

In SPM depth profiles from the Godavari delta (site 10, Fig. 1c), brGDGT concentrations varied from 1.2 to $4.0\,\mu g\,g^{-1}$ OC in the dry season ($n = 3$, three depths for one profile at the mid-river position), varied from 8.5 to $31.8\,\mu g\,g^{-1}$ OC in the wet season ($n = 9$, three depths for three profiles across the river), and showed no trend with depth (Fig. 3d, solid lines). Branched GDGT Ia was the most abundant compound, contributing 39 %–44 % in the dry season and 66 %–69 % to the total amount of brGDGTs in the wet season.

The relative abundances of individual brGDGTs showed minor variation with depth in both seasons. The contribution of 6-methyl brGDGTs varied between 30 % and 37 % in the dry and 14 % and 17 % in the wet season. In the middle Godavari (site 28; Fig. 1b), SPM depth profiles were only collected in the wet season. There, brGDGT concentrations ranged from 5.9 to $12.2\,\mu g\,g^{-1}$ OC ($n = 5$) (Fig. 3d, dashed lines), with brGDGT Ia as most abundant compound (53 %–55 %). The contribution of 6-methyl brGDGTs was 25 %–27 %. Also, the relative abundance of isoGDGTs showed little variation with depth at all sites and in both seasons, but $f(\text{cren}')$ and GDGT-0 / crenarchaeol were both lower in the dry season (0.03–0.04 and 0.27–0.36) than in the wet season (0.05–0.08 and 0.72–0.92).

4.2.4 GDGTs in riverbed sediments

Branched GDGTs were detected in all bulk riverbed sediments collected in the dry ($n = 37$) and wet season ($n = 37$), as well as in the fine fraction of the sediments sampled in the wet season ($n = 25$). Like in the Godavari soils, the contribution of brGDGTs IIb, IIc, IIc′, IIIa, IIIb, IIIb′, IIIc, and IIIc′ rarely exceeded 2 % (Fig. 4a). In the dry season, brGDGT concentrations ranged from 2.4 to $85.0\,\mu g\,g^{-1}$ OC (16.6 ± 2.4), with higher concentrations in the upper basin (26.8 ± 5.7, $n = 13$) than in the lower basin (11.1 ± 1.1, $n = 24$, $p \leq 0.02$) (Fig. 2d). Branched GDGT Ia was generally the most abundant compound (18 %–62 %, 39 ± 2 %), and its relative abundance was significantly lower in the upper basin (30 ± 1 %) than in the lower basin (44 ± 2 %, $p \leq 0.001$) (Figs. 2h, 4a, d). Branched GDGT IIa′ showed an opposite spatial trend and was significantly more abundant in the upper basin (23 ± 2 %) than in the lower basin (15 ± 1 %, $p \leq 0.001$) (Fig. 2i). The contribution of 6-methyl isomers was higher in the upper basin (43 ± 2 %) than the lower basin (30 ± 2 %, $p \leq 0.001$). Isoprenoid GDGT concentrations ranged from 0.8 to $39.3\,\mu g\,g^{-1}$ OC (6.7 ± 1.2), where GDGT-0 and crenarchaeol were the main compounds while GDGT-1, 2, and 3 and cren′ often contributed <5 %. Isoprenoid GDGT concentrations were higher in the upper basin ($10.0 \pm 2.8\,\mu g\,g^{-1}$ OC, $n = 12$) than in the lower basin ($5.0 \pm 0.8\,\mu g\,g^{-1}$ OC, $n = 24$) (Fig. 2k). Crenarchaeol was the most abundant isoGDGT in most riverbed sediments ($n = 24$), translating into BIT values of 0.51–1.00 (0.80 ± 0.02) with a higher average BIT value for the upper basin (0.86 ± 0.02) than the lower basin (0.76 ± 0.02, $p \leq 0.01$) (Fig. 2l). The $f(\text{cren}')$ ranged from 0.03–0.17, where the higher values mainly occurred in the upper basin (Fig. 2m). The ratio of GDGT-0 / crenarchaeol varied between 0.2 and 10.4 and was highest in the upper basin and sites with stagnant waters (Fig. 2n).

In the wet season, OC-normalised brGDGT concentrations in bulk sediments were on average ~ 2 times higher than in Godavari soils and similar to concentrations in wet-season SPM. Their concentrations varied between 1.2 and $36.9\,\mu g\,g^{-1}$ OC (12.5 ± 1.6, $n = 37$) and were higher in the upper basin (18.0 ± 3.8, $n = 8$) than in the lower basin (11.0 ± 1.6, $n = 29$) (Fig. 2d). Fine-fraction sediments had up to 10 times higher brGDGT concentrations than the bulk sediments from the same site (22.1 ± 1.4 vs. $13.1 \pm 1.7\,\mu g\,g^{-1}$ OC, $p \leq 0.001$, $n = 25$). The relative abundances were similar for fine and bulk sediments (Fig. 4a), and they are dominated by brGDGT Ia (21 %–77 %, 46 ± 2 %), except for site 42, where Ib dominated (Fig. 4a, d). The contribution of brGDGT Ia was substantially higher than in the dry season ($p \leq 0.02$) and generally increased downriver, resulting in a significantly lower relative abundance in the upper basin (33 ± 3 %, $n = 8$) than in the lower basin (50 ± 2 %, $n = 29$, $p \leq 0.001$) (Fig. 2h). Branched GDGT IIa′ showed the opposite spatial trend and

had a higher relative abundance in the upper basin (21 ± 2 %) than in the lower basin (13 ± 1 %, $p \leq 0.01$) (Fig. 2i). The contribution of 6-methyl isomers showed a similar trend as in Godavari soils and wet-season SPM but was on average lower than in the dry season ($p \leq 0.01$).

OC-normalized isoGDGT concentrations in wet-season bulk sediments ranged from 0.2 to 13.8 $\mu g\,g^{-1}$ OC (4.4 ± 0.6) (Fig. 2k), which is comparable to that of SPM collected during the same season. Fractional abundances of GDGT-1, 2, and 3 and cren′ were again often <5 %. BIT index values were 0.44–0.93 (0.78 ± 0.02) (Fig. 2l) and showed no distinct spatial trend, although they were remarkably high in the east tributaries (0.88–0.92, $n = 3$). For fine-fraction sediments, OC-normalized isoGDGT concentrations varied between 2.1 and 21.2 $\mu g\,g^{-1}$ OC (8.9 ± 0.8), which is almost double their average concentration in bulk sediments from the same sites (4.9 ± 0.7 $\mu g\,g^{-1}$ OC). BIT index values were 0.64–0.93 (0.79 ± 0.02), with the same trend as for the bulk sediments. The f(cren′) and GDGT-0 / crenarchaeol ratio values for fine-fraction sediments were similar to those of the bulk sediments (Fig. 2m, n).

4.2.5 GDGTs in Holocene Bay of Bengal sediments

All brGDGTs were detected in marine sediment core NGHP-01-16A spanning the Early to Late Holocene period ($n = 46$) (Fig. 4a) (Kirkels et al., 2021b). However, the contributions of IIc, IIIb, IIIb′, IIIc, and IIIc′ were always <1 %, and also IIb and IIc′ contributed mostly <2 % to the total brGDGT pool. The distribution of individual brGDGTs was mostly similar with depth but showed a slightly higher variability in the upper part of the core corresponding with the past ~2000 years (Fig. 5). In general, tetramethylated brGDGTs were the most abundant compounds (relative abundance 49 %–59 %), followed by pentamethylated (22 %–31 %) and hexamethylated brGDGTs (11 %–19 %). Branched GDGT Ia (32 %–40 %, average 37 ± 0 %) was the most abundant compound (Figs. 2h, 4a, e, 5b). Branched GDGT concentrations varied from 1.6 to 8.4 $\mu g\,g^{-1}$ OC (3.7 ± 0.2), without a clear trend with depth (Figs. 2d, 5b). The contribution of 6-methyl isomers ranged from 19 % to 26 % but was relatively invariant with depth. Isoprenoid GDGT concentrations were not quantified, but BIT index values ranged from 0.03 to 0.07 ($n = 38$; Figs. 2l, 5c), f(cren′) varied between 0.07 and 0.08, and GDGT-0 / crenarchaeol varied between 0.2 and 0.4, without a clear trend with depth (Fig. 2m, n).

5 Discussion

5.1 Temperature and moisture controls on GDGT distributions in Godavari soils

To determine the provenance of brGDGTs in the Godavari River and of those exported to the Bay of Bengal, we first investigate spatial variations in brGDGT distributions in surface soils across the basin. Branched GDGT Ia, which is typically associated with high temperatures in tropical to semi-arid regions (Weijers et al., 2007a; De Jonge et al., 2014a), is by far the most abundant compound in Godavari soils (Fig. 4a). The relative abundance of brGDGT Ia is higher in the upper than in the lower basin (Fig. 2h). Given the minor temperature variation across the Godavari basin (<3.5 °C), this suggests that its abundance is driven by another parameter than temperature. The relative abundances of all other brGDGTs vary considerably across the basin but do not show a clear spatial trend. A principal component analysis (PCA) of brGDGTs in Godavari soils reflects this variability in brGDGT distributions across the basin, as soils from the different subbasins are not restricted to single quadrants (Fig. 6a). Nevertheless, PC1 explains 50 % of the total variance and broadly separates soils from the east tributaries that load positive on PC1 with high relative abundances of brGDGT Ia, as well as from soils in the upper Godavari and north tributaries that have a negative loading on this PC and contain higher abundances of pentamethylated and hexamethylated brGDGTs, whereas soils from the middle and lower Godavari plot in the middle. Interestingly, most soils that plot negative on PC1 are formed on the Deccan basalts that underlie the upper basin, while those with positive loadings have developed on the felsic rocks in the lower basin. However, this separation is not consistent enough to link the different bedrock types to certain brGDGT distributions.

Although the BIT index is generally used to determine the relative contribution of terrestrial OC in a marine system, this index is sensitive to moisture availability in soils based on the observation that archaea that produce isoGDGTs, including crenarchaeol, appear to be better resistant to arid conditions than the bacteria that produce brGDGTs in dry, alkaline soils from China (Xie et al., 2012; Yang et al., 2014) and North America (Dirghangi et al., 2013). Hence, the relatively low BIT values in Godavari soils (0.52–0.91), especially in the upper basin, can be explained by the semi-arid to arid climate and slightly alkaline nature of the soils. However, there is no consistent spatial trend in the BIT index across the basin (Fig. 2j), indicating that the BIT index cannot be used to determine the provenance of brGDGTs carried by the Godavari River.

5.2 Identifying soil vs. aquatic sources of GDGTs in the Godavari River

To identify the areas of soil OC input into the Godavari River and the influence of (hydro)climate conditions under which soil OC is mobilised, the soil brGDGT distributions are compared with those in SPM and riverbed sediment collected in the dry and wet season. In contrast to the Godavari soils, a PCA of the relative abundances of eight major brGDGTs in SPM and bulk riverbed sediments collected in both seasons does reveal trends in brGDGT composition that can be linked to spatial and seasonal changes (Fig. 6b). PC1, explaining

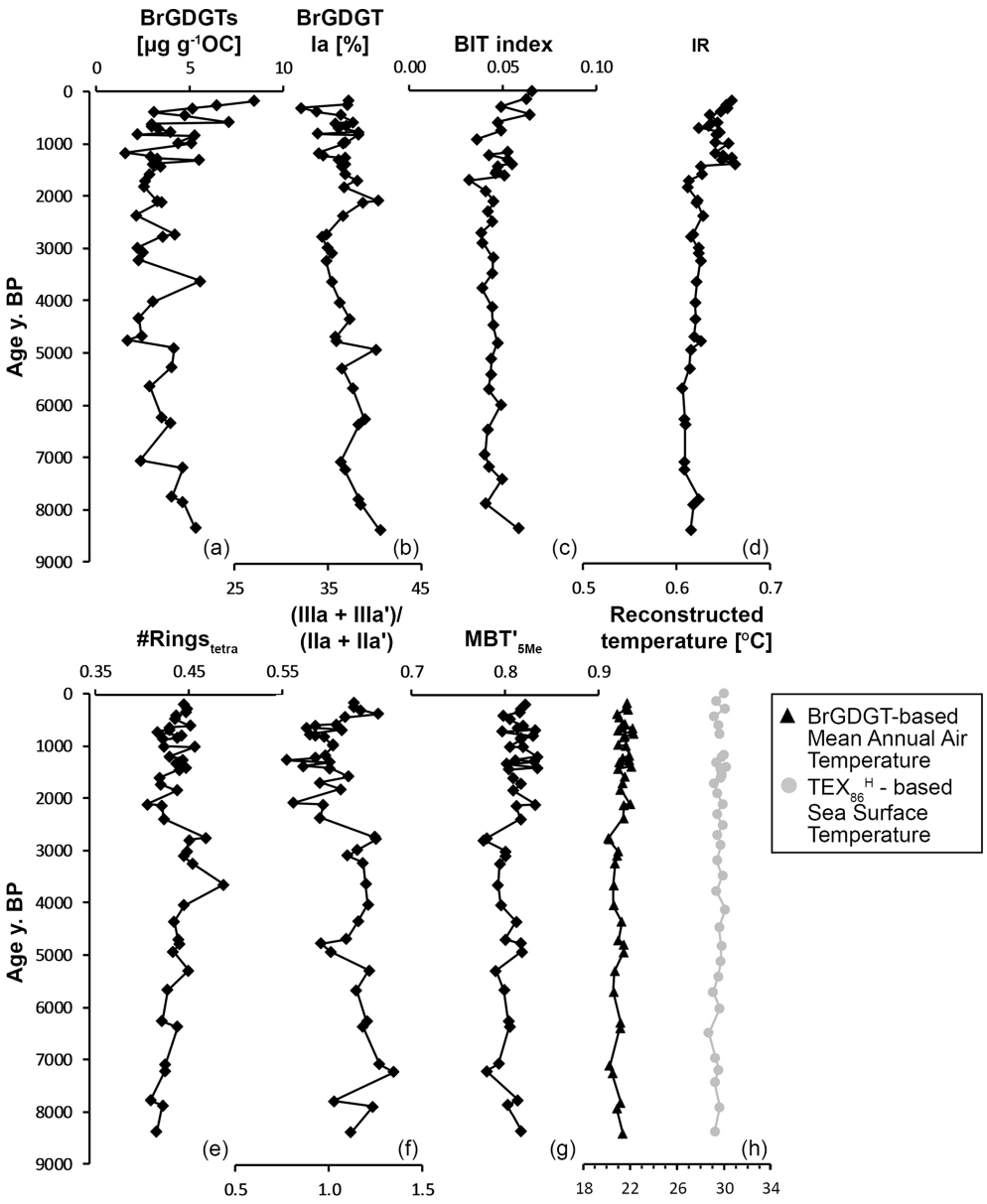

Figure 5. Branched and isoprenoid GDGTs and their indices in Holocene marine sediments of core NGHP-01-16A (∼ 1250 m water depth), retrieved ∼ 40 km from the Godavari River mouth in the Bay of Bengal. The age model from Usman et al. (2018) is used. **(a)** Concentration of brGDGTs, **(b)** relative abundance of Ia, **(c)** BIT index, **(d)** IR, **(e)** #rings$_{tetra}$, **(f)** (IIIa + IIIa′)/(IIa + IIa′) (following Xiao et al., 2016, 2020), **(g)** MBT′$_{5Me}$ index values, and **(h)** reconstructed temperatures (black triangles): continental MAAT, based on the MBT′$_{5Me}$ index and using the BayMBT$_0$ model of Dearing Crampton-Flood et al. (2020), and (grey circles) sea surface temperature, based on the TEX$^H_{86}$ index, following Kim et al. (2010). Note that the BIT index and SST records are at a slightly lower resolution ($n = 35$) than the brGDGT records ($n = 46$) due to the use of a different set of lipid extracts.

45.1 % of the total variance, clearly separates acyclic 5-methyl brGDGTs Ia, IIa, and IIIa from 6-methyl brGDGTs IIa′, IIb′, and IIIa′, as well as the upper and the lower basin. This suggests that the microbial community shifts from more 6-methyl brGDGT producers in the upper basin to a more 5-methyl-brGDGT-producing community in the lower basin. PC2, explaining 27.3 % of the total variance, seems to separate both the degree of methylation of brGDGTs and the degree of cyclisation, where brGDGTs without additional methylations but with one or two cyclopentane moieties plot positive on PC2 (Fig. 6b). PC2 further teases apart SPM and riverbed sediments collected in the upper basin that have high relative abundances of brGDGT IIa′ and IIIa′ from those collected in the lower basin in the wet season, which are distinct by high relative abundances of tetramethylated brGDGTs. Together, PC1 and PC2 show that SPM and riverbed sedi-

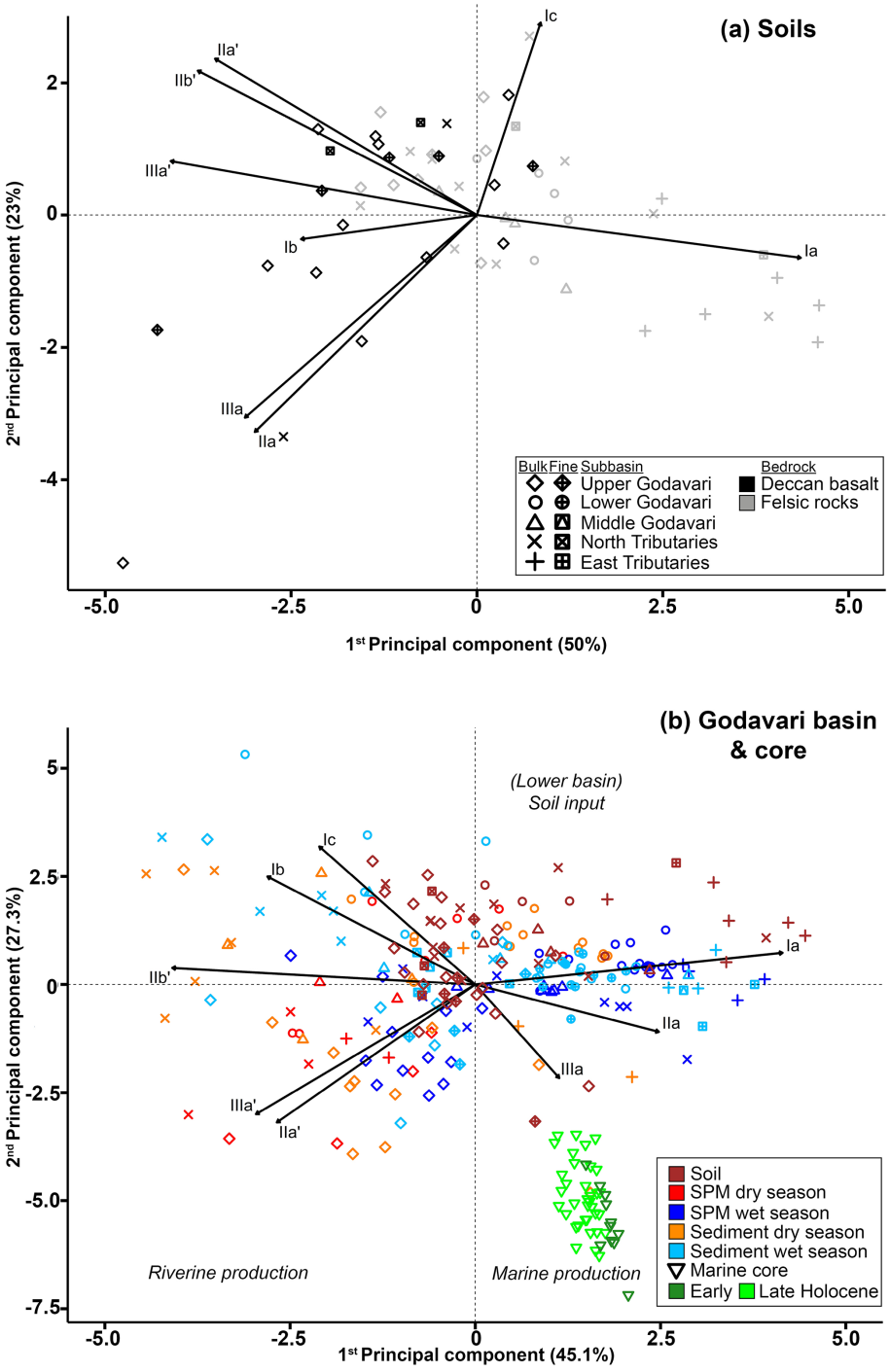

Figure 6. Principal component analysis (PCA) of the eight major brGDGTs (i.e. Ia, Ib, Ic, IIa, IIa′, IIb′, IIIa, and IIIa′). **(a)** PCA for soils formed on Deccan basalts (black) and felsic bedrock types (grey) (PC1 versus PC2). **(b)** PCA for SPM and bulk riverbed sediments collected in the wet and dry season (PC1 versus PC2), to which PCA scores of the bulk soils and Holocene marine sediments are added passively. The latter implies that the PCA calculation and biplot configuration is based on brGDGT distributions in river SPM and sediments (i.e. active samples), to which the scores of soils and marine sediments (i.e. passive samples) are added as an overlay. The vectors indicate the PCA scores of the individual brGDGTs. The symbols refer to the different subbasins and the different fractions (bulk and fine fractions $\leq 63\,\mu m$) (see legend **a**). The colours refer to the different sample types.

ments from the dry season as well as those collected in the upper basin are characterised by high relative abundances of 6-methyl brGDGTs, whereas SPM and sediments collected in the wet season in the lower basin are associated with more 5-methyl brGDGTs and specifically brGDGT Ia.

Passively adding the soil brGDGTs distributions to the PCA biplot based SPM and sediments shows that the soils mostly plot in the upper two quadrants and generally overlap with SPM and sediments collected in the lower basin in the wet season (Fig. 6b). Specifically, soils developed on felsic bedrock types in the lower basin plot in the right upper quadrant, together with SPM and sediments collected in the same part of the basin in the wet season. This similarity suggests that brGDGTs in this part of the Godavari River are most likely soil-derived. In contrast, the soils from the Deccan Plateau plot opposite to both wet- and dry-season SPM and sediments collected from the same region on PC2 (Fig. 6b). This difference is mainly driven by higher relative abundances of brGDGTs IIa′ and IIIa′ in SPM and sediments versus higher abundances of Ib and Ic in Deccan soils. This opposite loading on PC2 suggests that there is limited transfer of Deccan soils into the river or that soil-derived brGDGTs are overprinted by brGDGTs from other sources.

In general, SPM and sediments collected throughout the Godavari basin in the dry season, as well as those from the upper basin year-round, show relatively limited overlap with the soils (Fig. 6b). These samples are characterised by higher relative abundances of 6-methyl brGDGTs and brGDGT IIa′ in particular but lower abundances of Ia compared to soils (Figs. 2h, i, 4a–d). Indeed, IR values in dry-season SPM (0.88 ± 0.02, $p \leq 0.001$) and riverbed sediments (0.85 ± 0.01, $p \leq 0.001$), as well as SPM (0.90 ± 0.01, $p \leq 0.001$) and sediments (0.89 ± 0.02, $p \leq 0.05$) from the upper basin in both seasons, are significantly higher than those in soils (0.76 ± 0.02), suggesting that the brGDGTs in these subbasins and seasons are mainly produced in situ in the river (Figs. 2j, 7). Recent mesocosm experiments confirm that brGDGTs and 6-methyl brGDGTs in particular are produced in situ in the water column, especially at high(er) temperatures, high nutrient levels, and low-oxygen conditions (Martínez-Sosa and Tierney, 2019; Martínez-Sosa et al., 2020; Halamka et al., 2021). Similar conditions prevail in the Godavari basin in the dry season, when water temperatures are high ($\sim 29\,^{\circ}$C; Kirkels et al., 2020b), and nutrient inputs from agriculture and wastewater effluents facilitate phytoplankton production. The subsequent degradation of algal biomass consumes oxygen (Pradhan et al., 2014), creating the low-oxygen conditions favourable for brGDGT production. The low-oxygen conditions are supported by the elevated ratio of GDGT-0 / crenarchaeol in SPM and riverbed sediments, indicating the presence of methanogenic archaea, especially in the upper basin (Fig. 2n), and low suspended sediment loads and relatively high %OC in the Godavari River in the dry season (Fig. 2a, b) suggest that soil input is low and waters are non-turbid. Similarly, Kirkels et al. (2020a) reported that a decrease in turbidity in the dry season in an upper Amazon tributary promoted increased production of heterotrophic brGDGT-producing bacteria. The same scenario has also been used to explain brGDGT production behind dams in the Yangtze (Yang et al., 2013) and Danube (Freymond et al., 2017) rivers, where the reduced flow velocity and turbidity facilitated aquatic brGDGT production. Also, the isoGDGTs in the Godavari river have a mostly aquatic origin indicated by $f(\text{cren}')$ that is lower in SPM and riverbed sediments than in soils (Fig. 2m). This implies that isoGDGTs in the river are mostly produced by group I.1a Thaumarchaeota that produce relatively little cren′, whereas the isoGDGTs in soils are derived from group I.1b Thaumarchaeota that correspond with higher $f(\text{cren}')$ values (Pitcher et al., 2010, 2011; Kim et al 2012; Sinninghe Damsté et al., 2012; Elling et al., 2017; Bale et al., 2019). Notably, OC-normalised brGDGT and isoGDGT concentrations in Godavari riverbed sediments are ~ 2 times higher than in SPM in the dry season, especially in the upper basin (Fig. 2d, k). This suggests that GDGTs may also be produced in the sediment, although the overlap of SPM and sediments from the upper basin in the PCA biplot (Fig. 6b) could also be interpreted as preservation of GDGTs in the sediment layer.

In contrast to in the dry season, brGDGT distributions in SPM and riverbed sediments collected from the lower basin in the wet season resemble that of Godavari soils (Figs. 2h, 4a–c). This suggests that soil OC is mobilised and transferred into the Godavari River in the lower basin. Indeed, the IR of wet-season SPM (0.80 ± 0.01) and sediments (0.81 ± 0.02) from the lower basin is lower than in the dry season (SPM: 0.88 ± 0.02; sediment: 0.84 ± 0.02) and instead resembles that of soils (0.76 ± 0.02) (Figs. 2j, 7). In contrast, the IR remains significantly higher for wet-season SPM and sediments in the upper basin ($p \leq 0.05$), suggesting that brGDGTs in the upper basin have a predominantly aquatic source year-round. Indeed, the GDGT-0 / crenarchaeol in SPM and riverbed sediments from the upper basin remains high in the wet season (2.6 ± 0.4 and 1.2 ± 0.3, respectively), indicating that low-oxygen conditions suitable for brGDGT production prevailed, whereas this ratio is substantially lower in SPM and riverbed sediments from the lower basin (1.0 ± 0.1 and 0.8 ± 0.1, respectively) (Fig. 2n). The $f(\text{cren}')$ is always lower in SPM and riverbed sediments than in soils from the same subbasin, suggesting that isoGDGTs in the Godavari River always have a mostly aquatic source (Fig. 2n).

The change in brGDGT sources from the upper basin to the lower basin in the wet season reflects the precipitation pattern that was established based on water isotopes of Godavari river water in the year of sampling (Kirkels et al., 2020b). The lower basin and especially the north and east tributary regions received the most precipitation, thus promoting soil mobilisation, whereas the upper basin experienced a severe precipitation deficit that hampered soil mo-

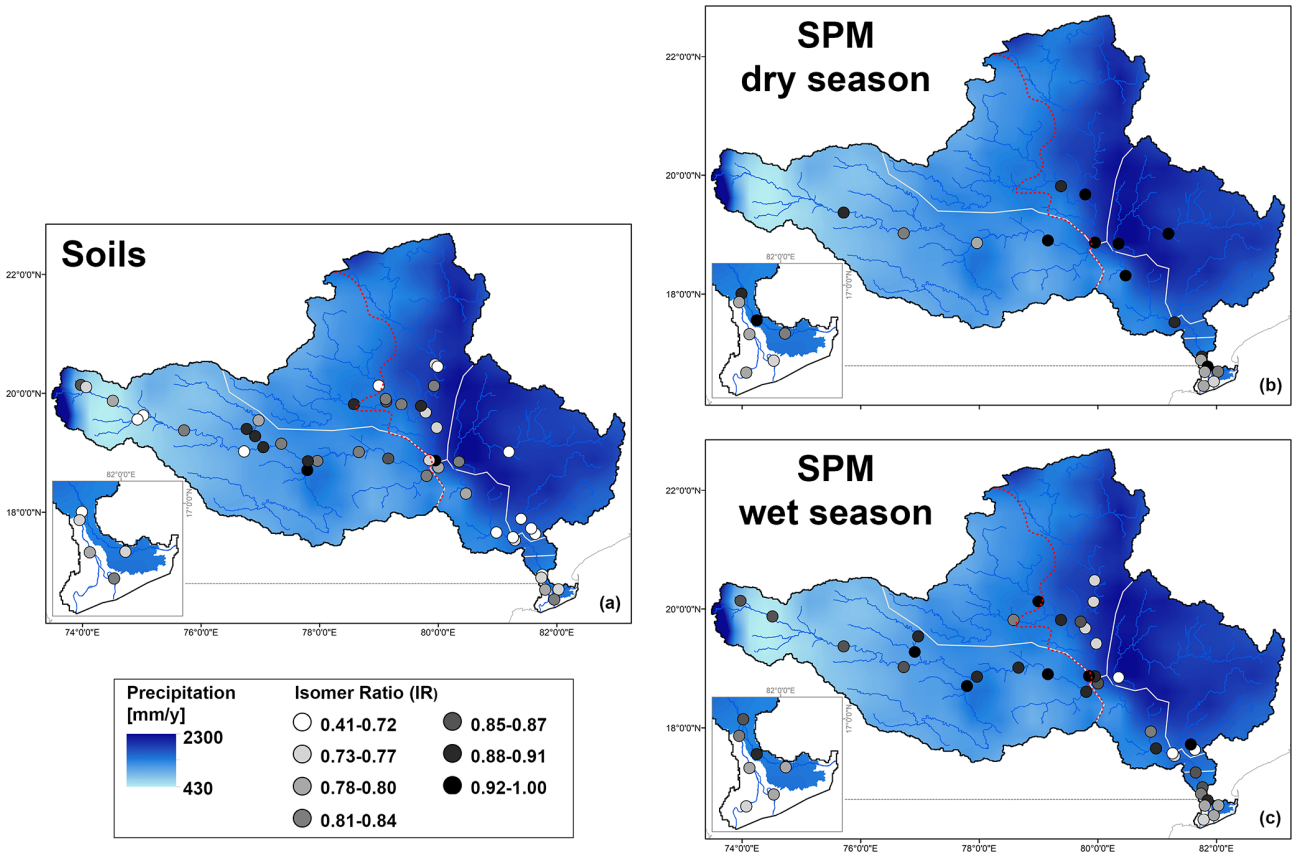

Figure 7. Maps showing the spatial distribution of IR values for **(a)** soils and SPM collected in the **(b)** dry and **(c)** wet season. The main panel shows the whole basin, with a zoom for the delta region. The points refer to the IR values, and the long-term average rainfall distribution is shown in the background.

bilisation and downstream transport (Fig. 1d). In addition, abundant dams in the upper basin reduce the river flow and create stagnant waters that facilitate aquatic productivity year-round (Pradhan et al., 2014; Kirkels et al., 2020b). The in situ production of brGDGTs in the upper basin results in significantly higher BIT index values for both wet-season (0.87 ± 0.02, $p \leq 0.05$) and dry-season (0.91 ± 0.04, $p \leq 0.01$) SPM compared to for the lower basin (wet season: 0.83 ± 0.01; dry season: 0.76 ± 0.05) (Fig. 2j). This contrasts with whitewater rivers carrying high suspended sediment loads in the lower Amazon basin, where BIT index values were found to decrease in the dry season as a result of crenarchaeol production in the river (Kim et al., 2012; Zell et al., 2013a). A possible explanation for the opposite trend in BIT index is that the production of crenarchaeol by ammonia-oxidising archaea in the lower Amazon depends on phytoplankton blooms to release N, whereas N levels are continuously high in the upper basin of the Godavari River (Gupta et al., 1997; Pradhan et al., 2014). Hence, it seems that the presence of stagnant waters and high nutrient levels may be important factors in determining whether conditions are favourable for the production of (6-methyl) brGDGTs or crenarchaeol in rivers and thus affect the BIT index.

Interestingly, prior to reaching the river mouth, the seasonal variation in brGDGT sources and distributions seems to be partly smoothened by the Rajahmundry reservoir lake that controls the discharge to the Godavari delta. The SPM and sediments collected downstream of the reservoir all plot positive on PC2 (Fig. 6b), representing a mixture of soil-derived brGDGTs (characterised by Ia) transported from the north and east tributaries in the wet season and aquatically produced brGDGTs (6-methyl brGDGTs) from the dry season.

5.3 Modes of soil OC transport through the modern Godavari basin

5.3.1 Lower basin as dominant sediment source

In order to assess whether brGDGTs are transported free or associated to mineral surfaces, we first determine the elemental composition of mineral particles in soils and riverbed sediments across the Godavari basin. The two distinct lithological units of the Godavari basin, i.e. Deccan basalts mainly in

the upper basin and the felsic metamorphic and sedimentary rocks in the lower basin (Fig. 1e), are reflected in the elemental composition of the soils. Concentrations of both Ti and Fe are significantly higher in soils from the Deccan region than in the felsic region. This difference can be explained by the presence of Ti- and Fe-oxydydrates in the Deccan basalts. In contrast, K concentrations are significantly higher in the felsic region, linked to the abundance of K-feldspars in these felsic bedrock types. The transition in bedrock composition is reflected in the trend in Ti/K and Fe/K ratios of the soils (Figs. 8a, A2), which match known endmember values for the Deccan basalts (Ti/K: 2.79; Fe/K: 18.13; Das and Krishnaswami, 2007) and felsic bedrock types (Ti/K: 0.21; Fe/K: 1.10; Moyen et al., 2003) in the basin. This implies that these ratios can be used to trace sediment provenance in the Godavari basin. Ti/K and Fe/K ratios have previously been used to reconstruct hydroclimate-related changes in chemical weathering intensity in the Mekong (Jiwarungrueangkul et al., 2019), Nile (Bastian et al., 2017), and Zambezi (Just et al., 2014) river basins, as well as to trace Andean inputs in modern riverbed sediments of the lower Amazon River (Häggi et al., 2016), its proximal fan (Govin et al., 2012, 2014), and in shelf sediments along the Chilean coast (Stuut et al., 2007). In the Godavari basin, Ti/K and Fe/K ratios of bulk sediments clearly decrease from the Deccan basalts region to the lower basin (felsic bedrock types) (Figs. 8b, c, A2). Notably, the bulk sediments in the dry and wet season show an abrupt change in elemental ratio values to the felsic endmember ~ 700 km from the river mouth. The fact that ratios are broadly similar for soils and riverbed sediments from the same location suggests that the sediments have a predominantly local/regional provenance. This implies that Deccan-derived material is not transported to the lower basin (Fig. 8b, c), probably as result of sediment trapping by the abundant dams in the upper basin and limited rainfall in the year of sample collection. The local, felsic origin of riverbed sediments in the lower basin and delta of the modern Godavari River is also confirmed by their neodymium isotopic composition (εNd; Ahmad et al., 2009). In addition, Ti/K and Fe/K ratios in marine cores covering the past ~ 300 years taken in front of the Godavari River mouth (Kalesha et al., 1980) closely match the endmember values for felsic bedrock types as well as those of the modern riverbed sediments in the lower basin (Figs. 8b, c, A2). Taken together, this indicates that the felsic bedrock region has been the dominant source of fluvial sediment delivered to the adjacent continental margin over the last centuries.

5.3.2 Links between bulk OC, soil-derived brGDGT, and mineral transport

To investigate possible protection and/or preferential transport of OC and soil-derived brGDGTs through the Godavari River resulting from associations with mineral particles, % OC and brGDGT distributions are first normalised to the Al/Si ratio. This normalisation helps to account for the change in bedrock geology in the Godavari basin, which may result in differences in grain size upon weathering (Figs. 8d–i, A3). Al is typically enriched in clays, which are also characterised by a high surface area. On the other hand, felsic bedrock weathers into Si-enriched, coarse-grained, low-mineral-surface-area material. The Al/Si ratio can thus serve as a proxy for the abundance of fine-grained, high-surface-area aluminosilicates that can host OC (Galy et al., 2008, 2010). For example, strong physical associations between OC and minerals were inferred from positive linear correlations between % OC and Al/Si in the Amazon and Ganges–Brahmaputra rivers (Galy et al., 2007, 2008, 2010; Bouchez et al., 2014; Häggi et al., 2016). This positive correlation revealed that mineral particles and OC respond in the same way across a range of bedrock types and seasonally contrasting hydrological conditions. At a molecular level, a similarly positive correlation between lignin concentrations and Al/Si in the Amazon basin showed that lignin was preferentially associated with fine-grained sediments (Sun et al., 2017). In contrast, *n*-alkanes that are also derived from vascular plants and were extracted from the same material did not show this correlation, which was explained by different source areas of *n*-alkanes and mineral particles (Häggi et al., 2016). In addition, the different behaviour of lignin and *n*-alkanes in the same river system suggests that molecular level OC sorting may take place during land–sea transfer, possibly depending on the properties of the molecule. In the Godavari basin, the %OC of dry-season riverbed sediments only shows a weak trend with Al/Si ($R^2 = 0.48$, Fig. 8e), indicating that OC was not closely associated with mineral particles. In the wet season, the % OC of riverbed sediments does show a positive linear correlation with Al/Si ($R^2 = 0.71$, Fig. 8f), revealing that bulk OC and mineral particles are transported together, possibly as a result of close OC–mineral association. A similar relation between brGDGT concentrations and Al/Si ratios would reveal if brGDGTs are also associated with mineral particles during river transport and support their use as tracers for soil OC. Like bulk OC, brGDGT concentrations in riverbed sediments show a weak relation with Al/Si in the dry season ($R^2 = 0.54$), excluding one outlier (site 47, in the arid, upper basin) that had exceptionally high brGDGT concentrations (Fig. 8h). Branched GDGT concentrations in riverbed sediments collected in the wet season reveal a somewhat stronger correlation with Al/Si ($R^2 = 0.60$) (Fig. 8i), although this correlation is still weaker than that for bulk OC and Al/Si (Fig. 8f, i). This difference suggests that brGDGTs may be less (strongly) associated with mineral particles than bulk OC. Indeed, earlier studies have suggested that brGDGT–mineral associations are continuously renewed and/or replaced by aquatic production or by local inputs during river transit (Li et al., 2015; Freymond et al., 2017, 2018b). Partitioning of brGDGTs into colloids, where they are dispersed in the river water but not directly associated with mineral surfaces, or preferential degradation of

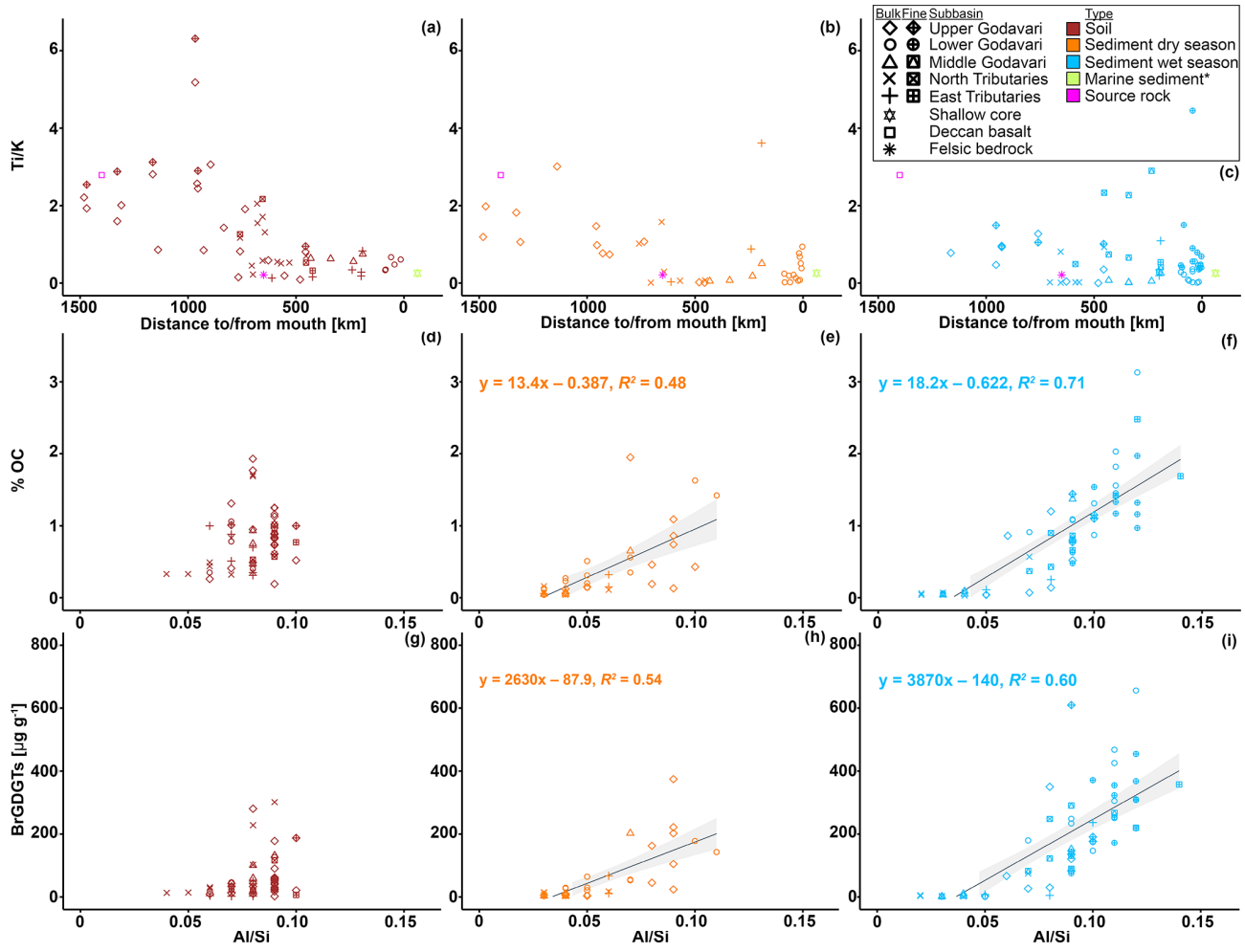

Figure 8. Ti/K ratios in **(a)** soils and riverbed sediments collected in the **(b)** dry and **(c)** wet season versus distance to/from the river mouth. The square and star (magenta) represent the endmember values for the Deccan basalts (Das and Krishnaswami, 2007) and felsic bedrock types (Archean Proterozoic gneiss complexes, APGC) (Moyen et al., 2003), respectively. The outlined star (green yellow) represents the average of marine sediments retrieved from * shallow cores in front of the Godavari mouth (0–48 cm b.s.f., ∼ 300 years; Kalesha et al., 1980) (error bars representing the standard deviation (± 0.02) are not visible as they are smaller than the symbol). The % OC and brGDGT concentrations versus Al/Si ratios in soils **(d, g)** and riverbed sediments collected in the **(e, h)** dry and **(f, i)** wet season, respectively. Low Al/Si ratios indicate a bulk mineralogical composition with high proportions of quartz (coarse grained), and high ratios indicate high proportions of micas and clays (fine grained) (Galy et al., 2008, 2010). Linear correlations (solid line) and 95 % confidence intervals (grey shading) are shown. The symbols refer to the different subbasins and the different fractions (bulk and fine fractions ≤ 63 µm). The colours refer to the different sample types.

brGDGTs over bulk OC could offer an alternative explanation for the slightly different trend of brGDGTs and bulk OC in the Godavari basin. Given the hydrophobic nature of brGDGTs, transition into the dissolved phase seems less likely.

Despite their weak link, both the mineral particles and the brGDGTs delivered to the modern-day river mouth appear to be sourced from the lower part of the Godavari basin. This is in contrast with other large river systems, where the provenance of these biomarkers and mineral particles seems more often decoupled. For instance, in the Amazon River, exported mineral fractions had an Andean signature, whereas brGDGTs in the lower Amazon and in the river fan sediments were sourced from lowland soil inputs and in situ production (Zell et al., 2013a, 2014b; van Soelen et al., 2017; Kirkels et al., 2020a). Similarly, in the Yangtze (Li et al., 2015) and Danube rivers (Freymond et al., 2018b), the upstream composition of the mineral fraction was preserved, while soil-derived brGDGTs seemed to be degraded in the river and then replaced by in situ-produced brGDGTs and/or local soil inputs with a different brGDGT distribution. The observed link between brGDGTs and sediment transport in the modern-day Godavari basin may be attributed to the rainfall distribution in the wet season that mobilises soils from

the lower basin and rapidly transports them downstream. The extreme turbidity and high flow velocities that characterise the Godavari River in the wet season furthermore limit autochthonous aquatic biological activity and in-river degradation (Gupta et al., 1997; Balakrishna and Probst, 2005; Syvitski and Saito, 2007). These conditions would likely hinder brGDGT production in the river and thus prevent overprinting of the soil-derived brGDGTs. Nevertheless, as soil brGDGT distributions do not significantly vary across the lower basin, it is not possible to fully exclude brGDGT replacement by local soil inputs during downstream transport.

5.3.3 Hydrodynamic sorting does not influence brGDGT distributions in the Godavari River

Hydrodynamic sorting effects within the river have been shown to result in a coarsening of SPM toward the riverbed, thereby affecting the depth distributions of % OC (Goñi et al., 2005; Galy et al., 2008; Bouchez et al., 2014; Guinoiseau et al., 2016) and lipid biomarkers (Kim et al., 2012; Feng et al., 2016; Feakins et al, 2018) that are associated with certain size fractions. Moreover, coarser and heavier mineral particles are preferentially deposited during sediment settling, favouring the transport of finer-grained sediments further downstream. Comparison of the % OC in the bulk and fine-fraction sediments collected in the wet season indicates that most OC is associated with the fine fraction in the Godavari sediments and may thus be susceptible to hydrodynamic sorting. Nevertheless, the % OC of SPM collected from several depth profiles in the middle Godavari (site 28) and the delta (site 10) is relatively invariant with depth (Figs. 1b, c, 3b). This finding is in contrast to other monsoonal rivers such as the Amazon (Bouchez et al., 2014; Kirkels et al., 2020a) and the Ganges–Brahmaputra River (Galy et al., 2008), where extensive size-related sorting is observed in the water column. In the Godavari River, only a slight drop in % OC of SPM (~ 1 % from the upper water column to close to the riverbed) occurred at the mid-channel position and near the eroding riverbank in the delta in the wet season, which suggests that occasional sorting may take place at peak discharge, albeit minor.

Like bulk OC, brGDGT concentrations in riverbed sediments are higher in fine-fraction sediments than in bulk sediments, even when normalised to % OC (Fig. 2b, d). The higher OC-normalised brGDGT concentrations in the fine fraction indicate that the grain size is important for the quantity of brGDGTs that is transported. However, brGDGT distributions and calculated proxy values are similar for fine-fraction and bulk sediments, suggesting that there is no selective sorting of certain brGDGTs (Figs. 2, 4). This observation confirms previous findings that brGDGT distributions are largely uniform among different size fractions in globally distributed river sediments (Peterse and Eglinton, 2017). Depth profiles of river SPM provide further support for the absence of sorting, as the concentration of brGDGTs, also when normalised to % OC, shows no pronounced trend with depth (Fig. 3d). Also, brGDGT distributions, here quantified in the IR, CBT′, and MBT'_{5Me} indices, are generally constant with depth and across the river in both the dry and wet season (Fig. 3f–h), similar to in the Danube (Freymond et al., 2018a) and the upper Amazon (Kirkels et al., 2020a). The homogeneous brGDGT distributions in sediment size fractions and depth profiles indicate that there is no hydrodynamic sorting effect on brGDGTs and no preferential transport (in the wet season) or production (in the dry season) of individual brGDGTs at a certain depth within the Godavari River. Consequently, the lower BIT index values in the delta in the dry season compared to in the wet season are not linked to preferential transport or production of brGDGTs and/or crenarchaeol (Fig. 3e) but related to reduced river discharge during the dry season (Kirkels et al., 2020b). The low discharge results in the intrusion of seawater that naturally contains higher concentrations of crenarchaeol compared to freshwater (Hopmans et al., 2004).

5.4 Connecting the Godavari River and the Bay of Bengal

5.4.1 Effective delta passage of soil-derived brGDGTs in the wet season

To evaluate the possible influence of salinity changes on brGDGT distributions, we target riverbed sediments collected along a transect in the main delta branch of the Godavari River. During the dry season, the salinity along this transect increased from ~ 25 to 29 psu towards the Godavari river mouth (Kirkels et al., 2020b). The brGDGT distributions in the sediments show a decrease in the relative abundances of 6-methyl brGDGTs IIa′ and IIIa′ compared to their 5-methyl counterparts IIa and IIIa. This trend resembles the strong shift from IIa′ and IIIa′ in the Yenisei River to more IIa and IIIa in the Kara Sea observed by De Jonge et al. (2015b). They attributed this change to rapid degradation of the labile, in-river-produced OC represented by 6-methyl brGDGTs, resulting in the relative enrichment of the initial (pre-aged) soil-derived brGDGT signal dominated by 5-methyl brGDGTs. The shift in brGDGT distributions along the salinity transect in the Godavari River delta corresponds with the extent of seawater intrusion (Kirkels et al., 2020b), suggesting that this change may be attributed to either marine brGDGT production and/or a loss of terrestrial and/or fluvial brGDGTs from mineral surfaces in this transition zone. Indeed, in the Yangtze River estuary, both processes were found to occur simultaneously in response to increasing salinity (Cao et al., 2022), and brGDGT production was also linked to the salinity gradient in Svalbard fjords (Dearing Crampton-Flood et al., 2019b). A potential loss of brGDGTs may be due to active OC processing at the freshwater–saltwater interface as well as to changes in ionic strength, which may reduce the binding of brGDGTs to min-

eral particles (e.g. Blattmann et al., 2019; Cao et al., 2022; Hou et al., 2020).

In contrast to in the dry season, brGDGT distributions do not change in the wet season, when the river plume extends beyond the Godavari mouth and the water is less saline (<3 psu) (Sridhar et al., 2008; Kirkels et al., 2020b). The seasonal difference in salinity indicates once more that the soil signal is only effectively exported to the Bay of Bengal in the wet season and supports previous studies that have shown that substantial soil mobilisation is needed (e.g. by a distinct season with increased precipitation) to export soil-derived brGDGTs downstream (Guo et al., 2020; Kirkels et al., 2020a; Märki et al., 2020). Nevertheless, given the reach of the transect, we cannot exclude that in the wet season, brGDGT distributions will be still affected by a salinity change further offshore.

5.4.2 Sources of brGDGTs in Bay of Bengal sediments

Branched GDGT distributions in a marine sediment core retrieved from the Bay of Bengal in front of the Godavari River mouth and spanning the Early to Late Holocene are distinctively different from those in the modern Godavari basin (Figs. 4a, 6b). Specifically, the Bay of Bengal core has lower relative abundances of 6-methyl brGDGTs, reflected by lower IR values of 0.61–0.66 (Figs. 2j, 5d). The relative abundances of IIIa and IIIa′ are higher than in most of the soils, SPM, and riverbed sediments from the Godavari basin (Fig. 4a). As a result, the Bay of Bengal core sediments are clearly separated from all other samples when they are passively added to the PCA of the brGDGTs in SPM and riverbed sediments from the modern Godavari basin (Fig. 6b). The distinct brGDGT distribution in the Bay of Bengal sediments from that in the modern Godavari basin points towards a different source of the brGDGTs. This implies that the majority of the soil-derived brGDGTs is not effectively transferred to the sedimentary archive and/or overprinted by marine in situ production during transport through the water column or after deposition on the sea floor. Low BIT index values in the Bay of Bengal core sediments (≤ 0.07; Figs. 2l, 5c) indicate that most of the OC in these sediments indeed has a marine origin. The limited contribution of terrestrial brGDGTs to the core location fits the observations of a rapid reduction in fluvially discharged brGDGTs offshore at, for example, the Siberian (Sparkes et al., 2015), Iberian (Zell et al., 2015; Warden et al., 2016), and East China continental shelf (Zhu et al., 2011).

The occurrence of marine in situ production of brGDGTs is increasingly recognised on continental margins, where it can be recognised based on a high degree of cyclisation of the tetramethylated brGDGTs (e.g. Peterse et al., 2009; Zhu et al., 2011; Zell et al., 2015; Sinninghe Damsté, 2016). Sinninghe Damsté (2016) defined $\#rings_{tetra} > 0.7$ as a cut-off value to identify a predominantly marine source of brGDGTs. However, the $\#rings_{tetra}$ in the Bay of Bengal core is relatively low (~ 0.29; Fig. 5e) and falls within the range covered by soils (0.36 ± 0.02), SPM (dry season: 0.37 ± 0.02; wet season: 0.25 ± 0.01), and riverbed sediments (dry season: 0.41 ± 0.02; wet season: 0.40 ± 0.03) in the modern Godavari basin. The increase in $\#rings_{tetra}$ in the marine realm is proposed to be a response to the relatively more alkaline conditions in the marine environment compared to those in soils (Sinninghe Damsté, 2016). Such a contrast is absent in the Godavari River system, where the pH of soils (~ 8) and seawater in the Bay of Bengal (~ 8.1) is similar (Sarma et al., 2015). Moreover, Sinninghe Damsté (2016) found that most brGDGT production takes place in the zone between 50–300 m water depth, whereas $\#rings_{tetra}$ appears to decrease again at greater water depths (Zell et al., 2015; Sinninghe Damsté, 2016). The latter is in agreement with the water depth of ~ 1250 m of the Bay of Bengal core. Indeed, recent studies investigating deep marine trenches (1.6–11 km), which hardly receive any terrestrial input, show a distinct brGDGT distribution from shallower marine sediments, and have lower values for $\#rings_{tetra}$ and IR (Xiao et al., 2020; Xu et al., 2020).

To further decipher the provenance of brGDGTs in the marine environment, Xiao et al. (2016) proposed that a ratio of (IIIa + IIIa′) / (IIa + IIa′) can be used. This ratio differentiates brGDGTs derived from soils, where this ratio is <0.6; from those produced in continental shelf sediments (≤ 5000 m water depth), where this ratio is mostly >1; and in deep (> 11 000 m) marine settings, where this ratio is >5 (Xiao et al., 2016, 2020; Xu et al., 2020). In the Bay of Bengal core, values for this ratio are mostly >1 (0.77–1.34, 1.07 ± 0.02; Fig. 5f) and are significantly higher than in soils (<0.20) and SPM and riverbed sediments (<0.33) from the modern Godavari basin in both seasons. This indicates that despite the low $\#rings_{tetra}$, the brGDGTs in the Bay of Bengal core do likely have a marine origin. Indeed, samples from the modern Godavari basin and the marine sediment core are clearly separated in a cross plot of the (IIIa + IIIa′) / (IIa + IIa′) ratio versus the relative abundance of IIIa′ (Fig. 9) and closely match the distinct trends of global soils and coastal shelf sediments.

5.4.3 Relatively ineffective transfer of soil-derived brGDGTs to Bay of Bengal sediments after fluvial discharge

The apparent absence of terrestrially derived brGDGTs in the Holocene Bay of Bengal sediment core contrasts with the presence of *n*-alkanoic acids derived from plant-wax lipids in the same sediments (Ponton et al., 2012; Usman et al., 2018). This discrepancy points towards different intrinsic stabilities, mineral binding, or transport mechanisms for these specific biomarkers. Similarly, Hou et al. (2020) reported that the burial efficiency of plant-derived *n*-alkanes differed from that of *n*-alkanoic acids in continental margin sediments in the South China Sea, revealing that these terrestrial

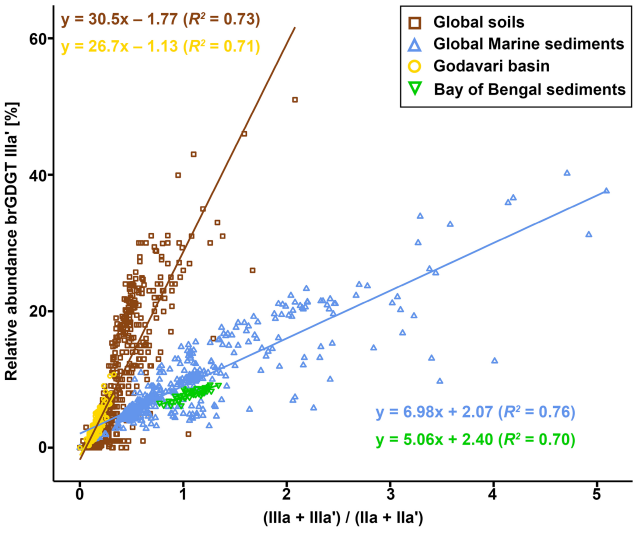

Figure 9. Cross plot of the ratio (IIIa + IIIa′) / (IIa + IIa′) versus the relative abundance of IIIa′ for globally distributed soils (square) and marine sediments (triangle) after Xiao et al. (2020) and Godavari basin samples, including soils, SPM, and riverbed sediments collected the dry and wet seasons (circle) and the Bay of Bengal Holocene sediments (inverted triangle). The solid lines denote the linear fit, and the correlations and R^2 are shown.

biomarker lipids have a distinct fate. In addition, different lipid biomarkers may derive from different parts of the river basin, as has been shown in the Danube (Freymond et al., 2018b) and Congo River basins (Hemingway et al., 2016), possibly linked to differences in their degree of binding in mineral associations and/or mode of transport (Eglinton et al., 2021).

In contrast to the modern Godavari basin, where sediment and brGDGT export is biased towards the lower basin, the elemental composition of the sediments in the upper part of the core that represents the Late Holocene is smectite-rich and indicates an origin from the Deccan basalts region in the upper Godavari basin (Giosan et al., 2017; Usman et al., 2018). However, smectite may be partially stripped of associated soil OC following changes in ionic composition and strength at the mouth-to-margin transition, where the mineral surfaces may be re-occupied by marine-produced OC (Blattmann et al., 2019). Since brGDGTs are presumably slightly less hydrophobic than plant-wax *n*-alkanoic acids, their association with mineral particles may be weaker. This could result in preferential loss of brGDGTs from mineral particles over *n*-alkanoic acids upon entering the marine realm and lead to differential settling, enrichment, and preservation of certain biomarkers in sedimentary archives (Blattmann et al., 2019).

When brGDGT concentrations are normalised to mineral surface area (MSA; data from Usman et al., 2018), they are 1 to 4 order(s) of magnitude lower than those of *n*-alkanoic acids in the same set of Godavari soils, dry-season riverbed sediments, and Holocene Bay of Bengal sediments. While *n*-alkanoic acid loadings remain in the same range along the soil-to-sea continuum (Usman et al., 2018), brGDGT loadings decrease on average by a factor ∼ 3 from the Godavari basin to the Bay of Bengal core (Fig. A3). This discrepancy indicates that these compounds have a different transfer and/or burial efficiency and would imply that the choice of biomarker that is used as specific tracer may influence estimates of the (long-term) sink capacity of marine sediments in the global C cycle, as well as their comparability in multi-proxy paleoreconstructions.

5.5 Implications for brGDGT-based paleoreconstructions

The inferred predominantly marine origin of brGDGTs in the Bay of Bengal sediments hampers their use as a paleothermometer for the nearby river catchment. Indeed, brGDGTs in the Bay of Bengal sediments translate into continental mean annual air temperatures (MAATs) between ∼ 20 and 22 °C (Fig. 5h), using the MBT'_{5Me} index and the $BayMBT_0$ model (Dearing Crampton-Flood et al., 2020). These reconstructed MAATs are lower than the basin-average, measured MAAT of ∼ 27 °C for the modern Godavari basin. Methods to correct for marine contributions to soil-derived brGDGTs based on the offset in $\#rings_{tetra}$ between marine sediments and catchments soils (Dearing Crampton-Flood et al., 2018) are not applicable to the Bay of Bengal core due to the water depth >1000 m of the site and the similar $\#rings_{tetra}$ in the Bay of Bengal core and the modern Godavari basin. Alternatively, the ratio proposed by Xiao et al. (2016, 2020) may be further explored to quantitatively assess the contribution of marine in situ production to the brGDGT pool in the core, provided that studies across environmental gradients confirm robust terrestrial, freshwater, and marine endmembers.

Interestingly, from ∼ 3000 years before the present there is a small change in the composition of brGDGTs in the core sediments, with slightly higher BIT, IR, and MBT'_{5Me} values and a lower relative abundance of brGDGT Ia, as well as $\#rings_{tetra}$ and (IIIa + IIIa′) / (IIa + IIa′) ratio values (Fig. 5b–g). This change corresponds with a steep increase in the sediment flux from the upper Godavari basin to the Bay of Bengal that was inferred from a change in detrital neodymium isotope values and the stable carbon isotopic composition of fatty acids (Giosan et al., 2017; Usman et al., 2018). This increase in soil erosion was attributed to natural causes such as aridification and a reduced vegetation cover and anthropogenic changes that resulted in increased agricultural land use and population expansion in the Godavari basin. The minor shift in brGDGT distributions could speculatively be linked to changes in the ratio of terrestrial-to-marine input. Alternatively, the shift may be explained by a change in the marine brGDGT-producing community, possibly in response to these changing inputs from the river system. Interestingly, the isoGDGTs preserved in the same core do not show this change in composition at ∼ 3000 years

before the present. Instead, they show that the sea surface temperatures (SST) consistently remained between ∼ 29 and 30 °C over the Holocene (Fig. 5h), similar to estimates based on Mg/Ca records in the western Bay of Bengal during the same period (Govil and Naidu, 2011). This observation would suggest that brGDGTs with a marine origin respond to different environmental forcing than isoGDGTs and/or are produced in a distinct part of the system, i.e. in sediments or the lower water column, instead of in (sub)surface waters.

Taken together, our study provides a clear example of the challenges when using brGDGTs as tracer for soil OC along the land–river–sea continuum or as a paleothermometer in marine sediments. Our findings support the statements of Dearing Crampton-Flood et al. (2021), who demonstrated the importance of determining the exact source(s) of brGDGTs prior to using them in temperature reconstructions, and highlight the need for more advanced methods to disentangle a mixed soil, fluvial, and marine in situ-produced brGDGT distribution in marine sediments.

6 Conclusions

Our comprehensive study of brGDGTs in soils, SPM, and riverbed sediments in the modern Godavari River basin allows us to trace soil OC along the entire soil–river–sea continuum. The hydrological contrasts between the dry and wet season, as well as spatially between the upper and lower basin linked to the natural change in bedrock geology, provide insight in the timing and source(s) of brGDGT and sediment transport through the Godavari River system. High contributions of 6-methyl brGDGTs in SPM and riverbed sediments indicate that brGDGTs are produced in situ in the river in the upper basin year-round and throughout the entire basin in the dry season. Elevated GDGT-0 / crenarchaeol ratio values at sites where the contribution of 6-methyl brGDGTs is high indicates that in situ production is favoured by low-oxygen conditions. Soil OC is only substantially mobilised and exported by the Godavari River to the Bay of Bengal in the wet season. The exported brGDGT distributions are biased towards the areas that receive the most precipitation in the lower part of the Godavari basin. This trend is amplified by the presence of dams that limit fluvial transport from the upper basin.

Comparison of the OC content, brGDGT concentrations, and distributions in soils and sediments with the elemental composition of the same soils and sediments indicates that bulk OC is transported in association with minerals, while brGDGTs may be less tightly bound to mineral particles. Regardless, sediments and brGDGTs share a common origin in the lower Godavari basin. However, this coupling may also result from the turbid conditions that hamper in situ production, in combination with rapid transport downriver linked to the high precipitation in the lower basin. River depth profiles and sediment size fractions reveal no hydrodynamic sorting effects on brGDGT distributions. Nevertheless, the fluvially discharged brGDGT distributions do not match those of brGDGTs in a Holocene sediment core retrieved in front of the Godavari mouth in the Bay of Bengal. This offset indicates that the soil-derived signal is rapidly lost after fluvial discharge and/or overprinted by marine in situ production. The observed disconnection between the Godavari basin and the Bay of Bengal sediments would impact brGDGT-based estimates of the capacity of marine sediments as a long-term sink for soil OC and also limit the use of brGDGTs in marine sediments for terrestrial paleoreconstructions.

Appendix A

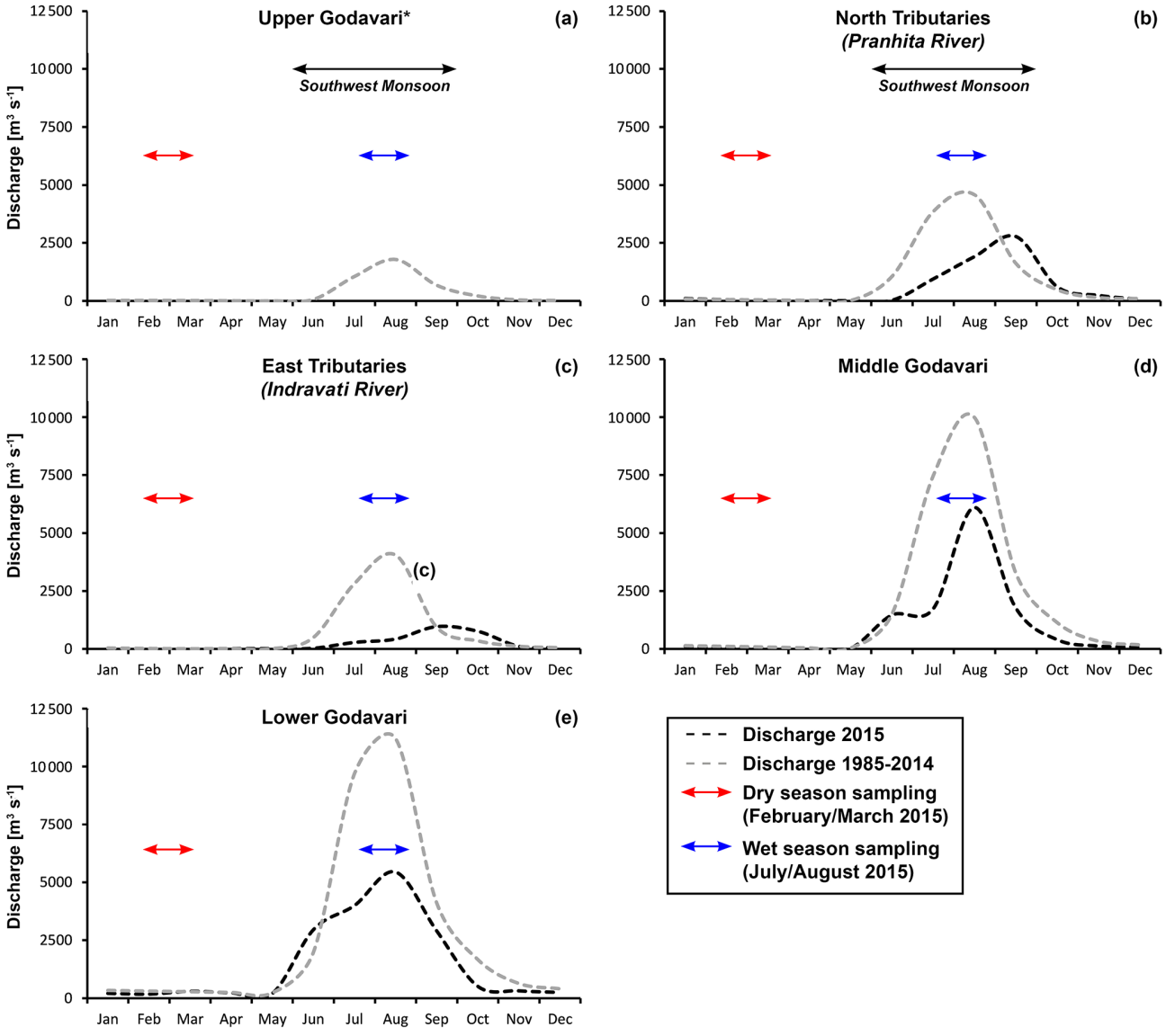

Figure A1. Monthly water discharge data for 2015 and the long-term average for 1985–2014 (India Water Resources Information System, 2021) for the Godavari subbasins, **(a)** upper Godavari (main stem, station at Mancherial, near site 31; * no data are available for April–December 2015), **(b)** north tributaries (Pranhita River, station at Tekra, near site 32), **(c)** east tributaries (Indravati River, station at Pathagudem, near site 26), **(d)** middle Godavari (main stem, station at Perur, ∼ 100 km upstream of site 28), and **(e)** lower Godavari (main stem, station at Polavaram, near site 13 (inflow of the reservoir lake at Rajahmundry)). The arrows indicate the period of sample collection in the dry season (red; February/March 2015) and in the wet season (blue; July/August 2015). The southwest monsoon (SWM) brings the majority of rainfall (75 %–85 %) in the period June–September. For rainfall distributions across the Godavari basin and variability in southwest monsoon precipitation, see Kirkels et al. (2020b).

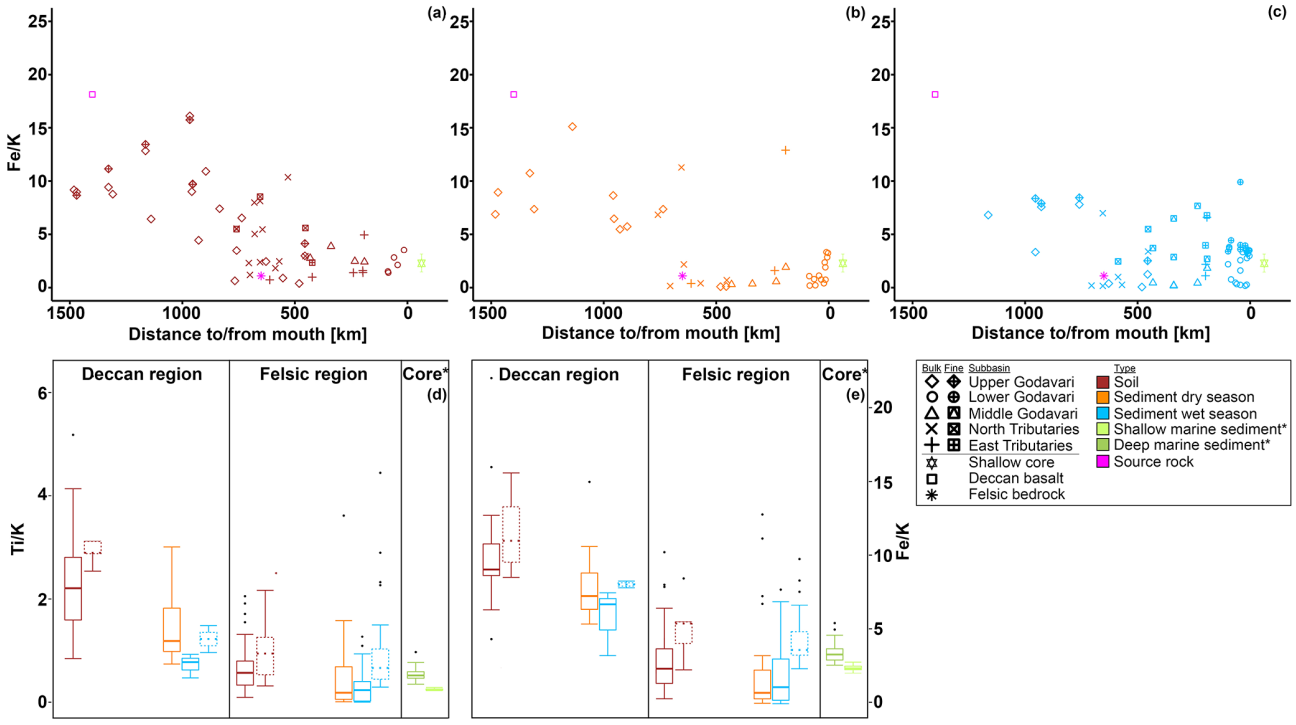

Figure A2. Fe/K ratios in **(a)** soils and riverbed sediments collected in the **(b)** dry and **(c)** wet season versus distance to/from the river mouth. The square and star (magenta) represent the endmember values for the Deccan basalts (Das and Krishnaswami, 2007) and felsic bedrock types (Archean Proterozoic Gneiss Complexes, APGC) (Moyen et al., 2003), respectively. The outlined star (green yellow) represents the average of marine sediments retrieved from shallow cores in front of the Godavari mouth (0–48 cm b.s.f., ∼ 300 years; Kalesha et al., 1980) (error bar represents the standard deviation: ± 0.83). Box-and-whisker plots of **(d)** Ti/K and **(e)** Fe/K ratios for the Godavari basin soils and sediments collected in the Deccan basalts and felsic regions and in marine sediments in the Bay of Bengal. * Core data are retrieved from shallow (0–48 cm b.s.f., ∼ 300 years; Kalesha et al., 1980) and deep marine sediments (0–300 m (NGHP-1-3B) and 0–184 m b.s.f. (NGHP-1-5C), no age model used; Mazumdar et al., 2015). The box represents the first (Q1) and third (Q3) quartiles, and the line in the box represents the median value; the whiskers extend to 1.5 × (Q3–Q1) values, and outliers are shown as points. Solid lines represent bulk data, and dashed lines represent the fine fractions (≤ 63 µm).

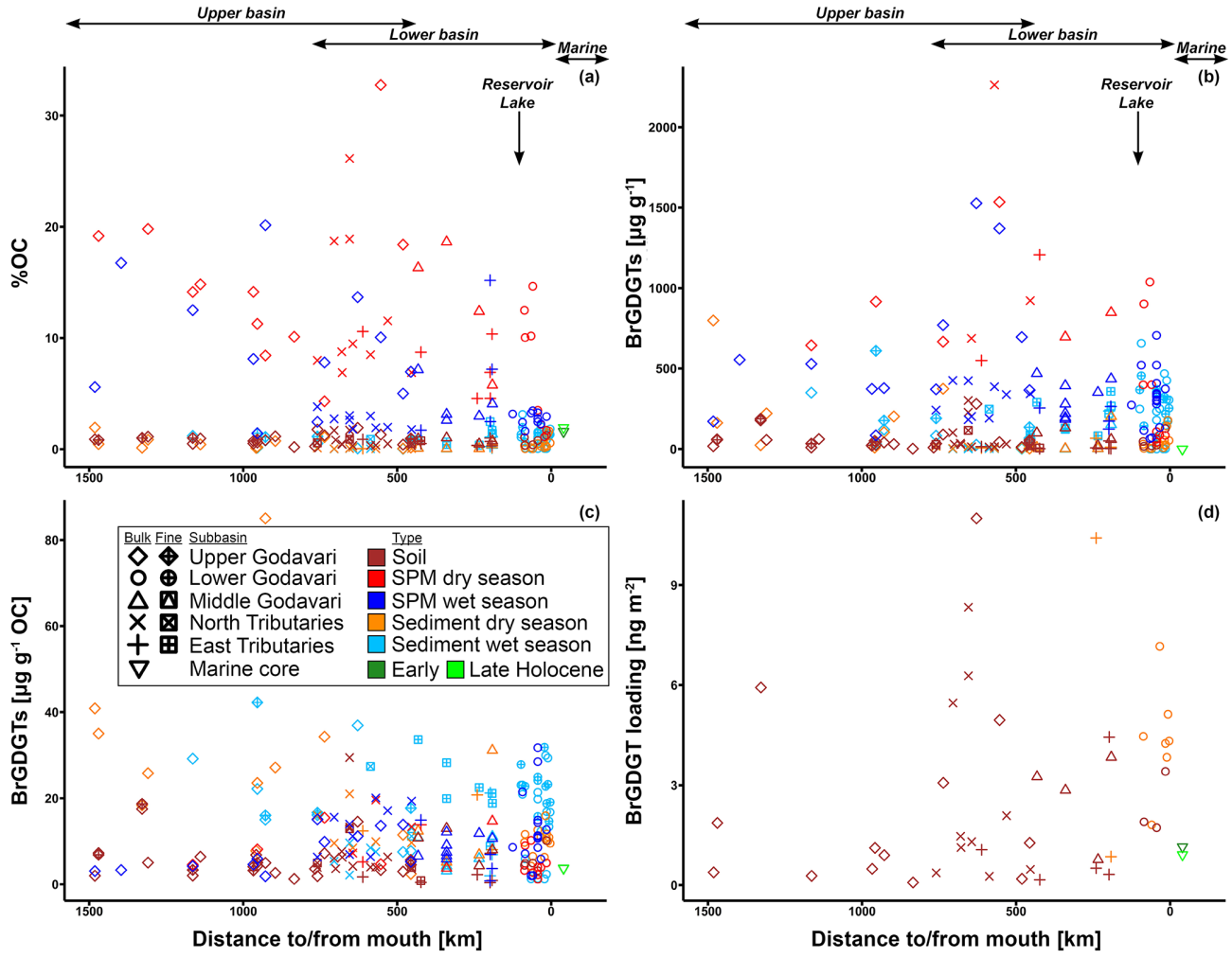

Figure A3. Evolution of % OC and brGDGTs along the Godavari River. **(a)** % OC; **(b)** brGDGT concentration normalised to sediment weight; **(c)** brGDGT concentration normalised to OC versus distance to/from the river mouth for soils, SPM, and riverbed sediments and average values for Holocene sediments in the marine realm (error bars ($\pm$ SE) are too small to be visible); and **(d)** brGDGT loadings, i.e. normalised to mineral surface area (MSA; see Usman et al., 2018) for Godavari soils ($n = 46$), riverbed sediments collected in the dry season ($n = 9$), and average values for Holocene sediments in the marine realm ($n = 46$; error bars ($\pm$ SE) are too small to be visible). The upper basin is defined as the upper Godavari and two sites (42 and 43, at 655 and 759 km from the mouth, respectively) in the north tributaries. The lower basin comprises the other north tributary sites, the east tributaries, and the middle and lower Godavari. The vertical arrow represents the location of the reservoir dam at Rajahmundry. The symbols refer to the different subbasins and the different fractions (bulk and fine fractions ≤ 63 µm). The colours refer to the different sample types.

Data availability. All geochemical and brGDGT data for the Godavari River basin are available in the Pangaea data repository and can be accessed at https://doi.org/10.1594/PANGAEA.934712 (Kirkels et al., 2021a). Isoprenoid GDGT data for the basin are available at https://doi.org/10.1594/PANGAEA.946817 (Kirkels et al., 2022). GDGT data for core NGHP-01-16 can be accessed at https://doi.org/10.1594/PANGAEA.934701 (Kirkels et al., 2021b). Branched GDGT data of the bulk soils are also accessible through https://doi.org/10.1594/PANGAEA.907818 (Dearing Crampton-Flood et al., 2019a).

Author contributions. FMSAK, TIE, and FP designed the study; FMSAK, HMZ, MOU, and FP planned and carried out fieldwork; CP and LG provided material from the Bay of Bengal core; FMSAK, HMZ, MOU, and CP carried out laboratory analyses; FMSAK, HMZ, SH, and FP interpreted the data; FMSAK took the lead in preparing the manuscript with input from all co-authors.

Competing interests. The contact author has declared that none of the authors has any competing interests.

Disclaimer. Publisher's note: Copernicus Publications remains neutral with regard to jurisdictional claims in published maps and institutional affiliations.

Acknowledgements. The fieldwork for this study was carried out with help from Prasanta Sanyal from the Indian Institute of Science Education and Research in Kolkata (India). We thank Maarten Lupker, Chris Martes, and Sayak Basu for their help with the premonsoon fieldwork campaign. For technical support in the laboratory, we thank Dominika Kasjaniuk, Anita van Leeuwen-Tolboom, Klaas Nierop, and Jan van Tongeren (general support and brGDGT analysis), and Coen Mulder (HF fumigation and ICP-MS) (Utrecht University, the Netherlands) as well as Ellen Hopmans and Marcel van der Mee (brGDGT and TOC analysis) (NIOZ, the Netherlands). We thank David Naafs and an anonymous reviewer for constructive feedback that has further improved the paper.

Financial support. This work was supported by the Netherlands Organisation for Scientific Research (NWO) (Veni grant no. 863.13.016 to FP).

Review statement. This paper was edited by Sebastian Naeher and reviewed by David Naafs and one anonymous referee.

References

Ahmad, S. M., Padmakumari, V. M., and Babu, G. A.: Strontium and neodymium isotopic compositions in sediments from Godavari, Krishna and Pennar rivers, Curr. Sci., 97, 1766–1769, 2009.

Amarasinghe, U., Chaudhuri, A., Collins, A. S., Deb, G., and Patranabis-Deb, S.: Evolving provenance in the Proterozoic Pranhita-Godavari Basin, India, Geosci. Front., 6, 453–463, 2015.

Aufdenkampe, A. K., Mayorga, E., Raymond, P. A., Melack, J. M., Doney, S. C., Alin, S. R., Aalto, R. E., and Yoo, K.: Riverine coupling of biogeochemical cycles between land, oceans, and atmosphere, Front. Ecol. Environ., 9, 53–60, 2011.

Babar, M. and Kaplay, R. D.: Godavari River: geomorphology and socio-economic characteristics, in: The Indian Rivers, edited by: Singh, D. S., Springer, Singapore, 319–337, ISBN: 978-981-10-9756-0, https://doi.org/10.1007/978-981-10-2984-4, 2018.

Babechuk, M. G., Widdowson, M., and Kamber, B. S.: Quantifying chemical weathering intensity and trace element release from two contrasting basalt profiles, Deccan Traps, India, Chem. Geol., 363, 56–75, 2014.

Balakrishna, K. and Probst, J.: Organic carbon transport and C/N ratio variations in a large tropical river: Godavari as a case study, India, Biogeochemistry, 73, 457–473, 2005.

Bale, N. J., Palatinszky, M., Rijpstra, W. I. C., Herbold, C. W., Wagner, M., and Sinninghe Damsté, J. S.: Membrane lipid composition of the moderately thermophilic ammonia-oxidizing archaeon "Candidatus Nitrosotenius uzonensis" at different growth temperatures, Appl. Environ. Microbiol. 85, e01332-19, https://doi.org/10.1128/AEM.01332-19, 2019.

Bastian, L., Revel, M., Bayon, G., Dufour, A., and Vigier, N.: Abrupt response of chemical weathering to Late Quaternary hydroclimate changes in northeast Africa, Sci. Rep., 7, 1–8, 2017.

Battin, T. J., Luyssaert, S., Kaplan, L. A., Aufdenkampe, A. K., Richter, A., and Tranvik, L. J.: The boundless carbon cycle, Nat. Geosci., 2, 598–600, 2009.

Bianchi, T. S.: The role of terrestrially derived organic carbon in the coastal ocean: A changing paradigm and the priming effect, P. Natl. Acad. Sci. USA, 108, 19473–19481, 2011.

Biksham, G. and Subramanian, V.: Elemental composition of Godavari sediments (central and southern Indian subcontinent), Chem. Geol., 70, 275–286, 1988a.

Biksham, G. and Subramanian, V.: Nature of solute transport in the Godavari basin, India, J. Hydrol., 103, 375–392, 1988b.

Biksham, G. and Subramanian, V.: Sediment transport of the Godavari River basin and its controlling factors, J. Hydrol., 101, 275–290, 1988c.

Blaga, C. I., Reichart, G. -J., Heiri, O., and Sinninghe Damsté, J. S.: Tetraether membrane lipid distributions in water-column particulate matter and sediments: a study of 47 European lakes along a north-south transect, J. Paleolimnol, 41, 523–540, 2009.

Blattmann, T. M., Liu, Z., Zhang, Y., Zhao, Y., Haghipour, N., Montluçon, D. B., Plötze, M., and Eglinton, T. I.: Mineralogical control on the fate of continentally derived organic matter in the ocean, Science, 366, 742–745, 2019.

Bouchez, J., Gaillardet, J., France-Lanord, C., Maurice, L., and Dutra-Maia, P.: Grain size control of river suspended sediment geochemistry: Clues from Amazon River depth profiles, Geochem. Geophys. Geosyst., 12, 1–24, 2011.

Bouchez, J., Galy, V., Hilton, R. G., Gaillardet, J., Moreira-Turcq, P., Pérez, M. A., France-Lanord, C., and Maurice, L.: Source, transport and fluxes of Amazon River particulate organic carbon: Insights from river sediment depth-profiles, Geochim. Cosmochim. Ac., 133, 280–298, 2014.

Butman, D. and Raymond, P. A.: Significant efflux of carbon dioxide from streams and rivers in the United States, Nat. Geosci., 4, 839–842, 2011.

Cao, J., Lian, E., Yang, S., Ge, H., Jin, X., He, J., and Jia, G.: The distribution of intact polar lipid-derived branched tetraethers along a freshwater-seawater pH gradient in coastal East China Sea, Chem. Geol., 596, 120808, https://doi.org/10.1016/j.chemgeo.2022.120808, 2022.

Cole, J. J., Prairie, Y. T., Caraco, N. F., McDowell, W. H., Tranvik, L. J., Striegl, R. G., Duarte, C. M., Kortelainen, P., Downing, J. A., and Middelburg, J. J.: Plumbing the global carbon cycle: integrating inland waters into the terrestrial carbon budget, Ecosystems, 10, 172–185, 2007.

Dang, X., Yang, H., Naafs, B. D. A., Pancost, R. D., and Xie, S.: Evidence of moisture control on the methylation of branched glycerol dialkyl glycerol tetraethers in semi-arid and arid soils, Geochim. Cosmochim. Ac., 189, 24–36, 2016.

Das, A. and Krishnaswami, S.: Elemental geochemistry of river sediments from the Deccan Traps, India: implications to sources

of elements and their mobility during basalt-water interaction, Chem. Geol., 242, 232–254, 2007.

Dearing Crampton-Flood, E., Peterse, F., Munsterman, D., and Sinninghe Damsté, J. S.: Using tetraether lipids archived in North Sea Basin sediments to extract North Western European Pliocene continental air temperatures, Earth Planet. Sci. Lett., 490, 193–205, 2018.

Dearing Crampton-Flood, E., Tierney, J. E., Peterse, F., Kirkels, F. M. S. A., and Sinninghe Damsté, J. S.: Global soil and peat branched GDGT compilation dataset, PANGAEA [data set], https://doi.org/10.1594/PANGAEA.907818, 2019a.

Dearing Crampton-Flood, E., Peterse, F., and Sinninghe Damsté, J. S.: Production of branched tetraethers in the marine realm: Svalbard fjord sediments revisited, Org. Geochem., 138, 103907, https://doi.org/10.1016/j.orggeochem.2019.103907, 2019b.

Dearing Crampton-Flood, E., Tierney, J. E., Peterse, F., Kirkels, F. M., and Sinninghe Damsté, J. S.: BayMBT: A Bayesian calibration model for branched glycerol dialkyl glycerol tetraethers in soils and peats, Geochim. Cosmochim. Ac., 268, 142–159, 2020.

Dearing Crampton-Flood, E., van der Weijst, C. M. H., van der Molen, G., Bouquet, M., Yedema, Y., Donders, T. H., Sangiorgi, F., Sluijs, A., Sinninghe Damsté, J. S., and Peterse, F.: Identifying marine and freshwater overprints on soil-derived branched GDGT temperature signals in Pliocene Mississippi and Amazon River fan sediments, Org. Geochem., 154, 1–11, 2021.

De Jonge, C., Hopmans, E. C., Stadnitskaia, A., Rijpstra, W. I. C., Hofland, R., Tegelaar, E., and Sinninghe Damsté, J. S.: Identification of novel penta- and hexamethylated branched glycerol dialkyl glycerol tetraethers in peat using HPLC–MS^2, GC–MS and GC–SMB-MS, Org. Geochem., 54, 78–82, 2013.

De Jonge, C., Hopmans, E. C., Zell, C. I., Kim, J., Schouten, S. and Sinninghe Damsté, J. S.: Occurrence and abundance of 6-methyl branched glycerol dialkyl glycerol tetraethers in soils: Implications for palaeoclimate reconstruction, Geochim. Cosmochim. Ac., 141, 97–112, 2014a.

De Jonge, C., Stadnitskaia, A., Hopmans, E. C., Cherkashov, G., Fedotov, A., and Sinninghe Damsté, J. S.: In situ produced branched glycerol dialkyl glycerol tetraethers in suspended particulate matter from the Yenisei River, Eastern Siberia, Geochim. Cosmochim. Ac., 125, 476–491, 2014b.

De Jonge, C., Stadnitskaia, A., Fedotov, A., and Sinninghe Damsté, J. S.: Impact of riverine suspended particulate matter on the branched glycerol dialkyl glycerol tetraether composition of lakes: The outflow of the Selenga River in Lake Baikal (Russia), Org. Geochem., 83–84, 241–252, 2015a.

De Jonge, C., Stadnitskaia, A., Hopmans, E. C., Cherkashov, G., Fedotov, A., Streletskaya, I. D., Vasiliev, A. A., and Sinninghe Damsté, J. S.: Drastic changes in the distribution of branched tetraether lipids in suspended matter and sediments from the Yenisei River and Kara Sea (Siberia): Implications for the use of brGDGT-based proxies in coastal marine sediments, Geochim. Cosmochim. Ac., 165, 200–225, 2015b.

Dirghangi, S. S., Pagani, M., Hren, M. T., and Tipple, B. J.: Distribution of glycerol dialkyl glycerol tetraethers in soils from two environmental transects in the USA, Org. Geochem., 59, 49–60, 2013.

Eglinton, T. I., Galy, V. V., Hemingway, J. D., Feng, X., Bao, H., Blattmann, T. M., Dickens, A. F., Gies, H., Giosan, L., and Haghipour, N.: Climate control on terrestrial biospheric carbon turnover, P. Natl. Acad. Sci. USA, 118, 1–9, 2021.

Elling, F. J., Könneke, M., Nicol, G. W., Stieglmeier, M., Bayer, B., Spieck, E., de la Torre, J. R., Becker, K. W., Thomm, M., Prosser, J. I., Herndl, G. J., Schleper, C., and Hinrichs, K. U.: Chemotaxonomic characterization of the thaumarchaeotal lipodome, Environ. Microbiol., 19, 2681–2700, 2017.

Feakins, S. J., Wu, M. S., Ponton, C., Galy, V., and West, A. J.: Dual isotope evidence for sedimentary integration of plant wax biomarkers across an Andes-Amazon elevation transect, Geochim. Cosmochim. Ac., 242, 64–81, 2018.

Feng, X., Feakins, S. J., Liu, Z., Ponton, C., Wang, R. Z., Karkabi, E., Galy, V., Berelson, W. M., Nottingham, A. T., and Meir, P.: Source to sink: Evolution of lignin composition in the Madre de Dios River system with connection to the Amazon basin and offshore, J. Geophys. Res.-Biogeo., 121, 1316–1338, 2016.

Freymond, C. V., Peterse, F., Fischer, L. V., Filip, F., Giosan, L., and Eglinton, T. I.: Branched GDGT signals in fluvial sediments of the Danube River basin: Method comparison and longitudinal evolution, Org. Geochem., 103, 88–96, 2017.

Freymond, C. V., Lupker, M., Peterse, F., Haghipour, N., Wacker, L., Filip, F., Giosan, L., and Eglinton, T. I.: Constraining instantaneous fluxes and integrated compositions of fluvially discharged organic matter, Geochem. Geophys. Geosyst., 19, 2453–2462, 2018a.

Freymond, C. V., Kündig, N., Stark, C., Peterse, F., Buggle, B., Lupker, M., Plötze, M., Blattmann, T. M., Filip, F., and Giosan, L.: Evolution of biomolecular loadings along a major river system, Geochim. Cosmochim. Ac., 223, 389–404, 2018b.

Friedlingstein, P., O'Sullivan, M., Jones, M. W., Andrew, R. M., Hauck, J., Olsen, A., Peters, G. P., Peters, W., Pongratz, J., Sitch, S., Le Quéré, C., Canadell, J. G., Ciais, P., Jackson, R. B., Alin, S., Aragão, L. E. O. C., Arneth, A., Arora, V., Bates, N. R., Becker, M., Benoit-Cattin, A., Bittig, H. C., Bopp, L., Bultan, S., Chandra, N., Chevallier, F., Chini, L. P., Evans, W., Florentie, L., Forster, P. M., Gasser, T., Gehlen, M., Gilfillan, D., Gkritzalis, T., Gregor, L., Gruber, N., Harris, I., Hartung, K., Haverd, V., Houghton, R. A., Ilyina, T., Jain, A. K., Joetzjer, E., Kadono, K., Kato, E., Kitidis, V., Korsbakken, J. I., Landschützer, P., Lefèvre, N., Lenton, A., Lienert, S., Liu, Z., Lombardozzi, D., Marland, G., Metzl, N., Munro, D. R., Nabel, J. E. M. S., Nakaoka, S.-I., Niwa, Y., O'Brien, K., Ono, T., Palmer, P. I., Pierrot, D., Poulter, B., Resplandy, L., Robertson, E., Rödenbeck, C., Schwinger, J., Séférian, R., Skjelvan, I., Smith, A. J. P., Sutton, A. J., Tanhua, T., Tans, P. P., Tian, H., Tilbrook, B., van der Werf, G., Vuichard, N., Walker, A. P., Wanninkhof, R., Watson, A. J., Willis, D., Wiltshire, A. J., Yuan, W., Yue, X., and Zaehle, S.: Global Carbon Budget 2020, Earth Syst. Sci. Data, 12, 3269–3340, https://doi.org/10.5194/essd-12-3269-2020, 2020.

Galy, V., France-Lanord, C., Beyssac, O., Faure, P., Kudrass, H., and Palhol, F.: Efficient organic carbon burial in the Bengal fan sustained by the Himalayan erosional system, Nature, 450, 407–411, 2007.

Galy, V., France-Lanord, C., and Lartiges, B.: Loading and fate of particulate organic carbon from the Himalaya to the Ganga–Brahmaputra delta, Geochim. Cosmochim. Ac., 72, 1767–1787, 2008.

Galy, V., France-Lanord, C., Beyssac, O., Lartiges, B., and Rhaman, M.: Organic carbon cycling during Himalayan erosion: pro-

cesses, fluxes and consequences for the global carbon cycle, in: Climate Change and Food Security in South Asia, edited by: Lal, R., Sivakumar, M., Faiz, S., Mustafizur Rahman, A., and Islam, K., Springer, Dordrecht, 163–181, ISBN: 978-90-481-9515-2, https://doi.org/10.1007/978-90-481-9516-9, 2010.

Galy, V., Peucker-Ehrenbrink, B., and Eglinton, T.: Global carbon export from the terrestrial biosphere controlled by erosion, Nature, 521, 204–207, 2015.

Giosan, L., Ponton, C., Usman, M., Blusztajn, J., Fuller, D. Q., Galy, V., Haghipour, N., Johnson, J. E., McIntyre, C., Wacker, L., and Eglinton, T. I.: Short communication: Massive erosion in monsoonal central India linked to late Holocene land cover degradation, Earth Surf. Dynam., 5, 781–789, https://doi.org/10.5194/esurf-5-781-2017, 2017.

Goñi, M. A., Cathey, M. W., Kim, Y. H., and Voulgaris, G.: Fluxes and sources of suspended organic matter in an estuarine turbidity maximum region during low discharge conditions, Estuar. Coast. Shelf Sci., 63, 683–700, 2005.

Govil, P. and Naidu, P. D.: Variations of Indian monsoon precipitation during the last 32 kyr reflected in the surface hydrography of the Western Bay of Bengal, Quat. Sci. Rev., 30, 3871–3879, 2011.

Govin, A., Holzwarth, U., Heslop, D., Ford Keeling, L., Zabel, M., Mulitza, S., Collins, J. A., and Chiessi, C. M.: Distribution of major elements in Atlantic surface sediments (36° N–49° S): Imprint of terrigenous input and continental weathering, Geochem. Geophys. Geosyst., 13, 1–23, 2012.

Govin, A., Chiessi, C. M., Zabel, M., Sawakuchi, A. O., Heslop, D., Hörner, T., Zhang, Y., and Mulitza, S.: Terrigenous input off northern South America driven by changes in Amazonian climate and the North Brazil Current retroflection during the last 250 ka, Clim. Past, 10, 843–862, https://doi.org/10.5194/cp-10-843-2014, 2014.

Guinoiseau, D., Bouchez, J., Gélabert, A., Louvat, P., Filizola, N., and Benedetti, M. F.: The geochemical filter of large river confluences, Chem. Geol., 441, 191–203, 2016.

Gunnell, Y.: Relief and climate in South Asia: the influence of the Western Ghats on the current climate pattern of peninsular India, Int. J. Climatol., 17, 1169–1182, 1997.

Guo, J., Glendell, M., Meersmans, J., Kirkels, F., Middelburg, J. J., and Peterse, F.: Assessing branched tetraether lipids as tracers of soil organic carbon transport through the Carminowe Creek catchment (southwest England), Biogeosciences, 17, 3183–3201, https://doi.org/10.5194/bg-17-3183-2020, 2020.

Gupta, L. P., Subramanian, V., and Ittekkot, V.: Biogeochemistry of particulate organic matter transported by the Godavari River, India, Biogeochemistry, 38, 103–128, 1997.

Häggi, C., Sawakuchi, A. O., Chiessi, C. M., Mulitza, S., Mollenhauer, G., Sawakuchi, H. O., Baker, P. A., Zabel, M., and Schefuß, E.: Origin, transport and deposition of leaf-wax biomarkers in the Amazon Basin and the adjacent Atlantic, Geochim. Cosmochim. Ac., 192, 149–165, 2016.

Halamka, T. A., McFarlin, J. M., Younkin, J. M., Depoy, A. D., Dildar, J., and Kopf, N.: Oxygen limitation can trigger the production of branched GDGTs in culture, Geochem. Pers. Letters 19, 36–39, 2021.

Hedges, J. I.: Global biogeochemical cycles: progress and problems, Mar. Chem., 39, 67–93, 1992.

Hedges, J. I. and Keil, R. G.: Sedimentary organic matter preservation: an assessment and speculative synthesis, Mar. Chem., 49, 81–115, 1995.

Hedges, J. I., Keil, R. G., and Benner, R.: What happens to terrestrial organic matter in the ocean?, Org. Geochem., 27, 195–212, 1997.

Hemingway, J. D., Schefuß, E., Dinga, B. J., Pryer, H., and Galy, V. V.: Multiple plant-wax compounds record differential sources and ecosystem structure in large river catchments, Geochim. Cosmochim. Ac., 184, 20–40, 2016.

Hemingway, J. D., Schefuß, E., Spencer, R. G., Dinga, B. J., Eglinton, T. I., McIntyre, C., and Galy, V. V.: Hydrologic controls on seasonal and inter-annual variability of Congo River particulate organic matter source and reservoir age, Chem. Geol., 466, 454–465, 2017.

Hemingway, J. D., Rothman, D. H., Grant, K. E., Rosengard, S. Z., Eglinton, T. I., Derry, L. A., and Galy, V. V.: Mineral protection regulates long-term global preservation of natural organic carbon, Nature, 570, 228–231, 2019.

Holtvoeth, J., Kolonic, S., and Wagner, T.: Soil organic matter as an important contributor to late Quaternary sediments of the tropical West African continental margin, Geochim. Cosmochim. Ac., 69, 2031–2041, 2005.

Hopmans, E. C., Weijers, J. W., Schefuß, E., Herfort, L., Sinninghe Damsté, J. S., and Schouten, S.: A novel proxy for terrestrial organic matter in sediments based on branched and isoprenoid tetraether lipids, Earth Planet. Sci. Lett., 224, 107–116, 2004.

Hopmans, E. C., Schouten, S., and Sinninghe Damsté, J. S.: The effect of improved chromatography on GDGT-based palaeoproxies, Org. Geochem., 93, 1–6, 2016.

Hou, P., Yu, M., Zhao, M., Montluçon, D. B., Su, C., and Eglinton, T. I.: Terrestrial biomolecular burial efficiencies on continental margins, J. Geophys. Res.-Biogeo., 125, 1–15, 2020.

Huguet, C., Hopmans, E. C., Febo-Ayala, W., Thompson, D. H., Sinninghe Damsté, J. S., and Schouten, S.: An improved method to determine the absolute abundance of glycerol dibiphytanyl glycerol tetraether lipids, Org. Geochem., 37, 1036–1041, 2006.

India Water Resources Information System, Government of India, Ministry of Jal Shatki, Department of Water Resources, River Development and Ganga Rejuvenation: Discharge data and water levels in the Godavari River basin, https://indiawris.gov.in/, last access: 1 July 2021.

Jiwarungrueangkul, T., Liu, Z., Stattegger, K., and Sang, P. N.: Reconstructing chemical weathering intensity in the Mekong River basin since the Last Glacial Maximum, Paleoceanogr. Paleoclimatol., 34, 1710–1725, 2019.

Just, J., Schefuß, E., Kuhlmann, H., Stuut, J. W., and Pätzold, J.: Climate induced sub-basin source-area shifts of Zambezi River sediments over the past 17 ka, Palaeogeogr. Palaeoclimatol. Palaeoecol., 410, 190–199, 2014.

Kalesha, M., Rao, K. S., and Somayajulu, B.: Deposition rates in the Godavari delta, Mar. Geol., 34, M57–M66, 1980.

Keil, R. G., Mayer, L. M., Quay, P. D., Richey, J. E., and Hedges, J. I.: Loss of organic matter from riverine particles in deltas, Geochim. Cosmochim. Ac., 61, 1507–1511, 1997.

Keller, G., Adatte, T., Gardin, S., Bartolini, A., and Bajpai, S.: Main Deccan volcanism phase ends near the K–T boundary: evidence from the Krishna–Godavari Basin, SE India, Earth Planet. Sci. Lett., 268, 293–311, 2008.

Kim, J. G., Jung, M. Y., Park, S. J., Rijpstra, W. I. C., Sinninghe Damsté, J. S., Madsen, E. L., Min, D., Kim, J. S., Kim, G. J., and Rhee, S. K.: Cultivation of a highly enriched ammonia-oxidizing archaeon of thaumarchaeotal group I.1b from an agricultural soil, Environ. Microbiol., 14, 1528–1543, 2012.

Kim, J. H., Van der Meer, J., Schouten, S., Helmke, P., Willmott, V., Sangiorgi, F., Koç, N., Hopmans, E. C., and Sinninghe Damsté, J. S.: New indices and calibrations derived from the distribution of crenarchaeal isoprenoid tetraether lipids: Implications for past sea surface temperature reconstructions, Geochim. Cosmochim. Ac., 74, 4639–4654, 2010.

Kim, J. H., Zell, C., Moreira-Turcq, P., Pérez, M. A., Abril, G., Mortillaro, J., Weijers, J. W., Meziane, T., and Sinninghe Damsté, J. S.: Tracing soil organic carbon in the lower Amazon River and its tributaries using GDGT distributions and bulk organic matter properties, Geochim. Cosmochim. Ac., 90, 163–180, 2012.

Kim, J. H., Ludwig, W., Buscail, R., Dorhout, D., and Sinninghe Damsté, J. S.: Tracing tetraether lipids from source to sink in the Rhône River system (NW Mediterranean), Front. Earth Sci., 3, 1–22, 2015.

Kirkels, F. M. S. A., Zwart, H., Usman, M., and Peterse, F.: Branched glycerol dialkyl glycerol tetraethers, crenarchaeol and geochemical parameters in soils, SPM and riverbed sediments in the Godavari River basin (India), PANGAEA [data set], https://doi.org/10.1594/PANGAEA.934712, 2021a.

Kirkels, F. M. S. A., Usman, M., Hou, S., Ponton, C., and Peterse, F.: Glycerol dialkyl glycerol tetraethers in a Holocene sediment core (NGHP-01-16A) in front of the Godavari River in the Bay of Bengal (India), PANGAEA [data set], https://doi.org/10.1594/PANGAEA.934701, 2021b.

Kirkels, F. M., Ponton, C., Galy, V., West, A. J., Feakins, S. J., and Peterse, F.: From Andes to Amazon: assessing branched tetraether lipids as tracers for soil organic carbon in the Madre de Dios River system, J. Geophys. Res.-Biogeo., 125, 1–18, 2020a.

Kirkels, F. M., Zwart, H. M., Basu, S., Usman, M. O., and Peterse, F.: Seasonal and spatial variability in δ^{18}O and δD values in waters of the Godavari River basin: insights into hydrological processes, J. Hydrol. Reg. Stud., 30, 1–25, 2020b.

Kirkels, F. M. S. A., Zwart, H., Usman, M. O., and Peterse, F.: Isoprenoid glycerol dialkyl glycerol tetraether (isoGDGT) lipids in soils, SPM, and riverbed sediments in the Godavari Basin (India), PANGAEA [data set], https://doi.org/10.1594/PANGAEA.946817, 2022.

Komada, T., Anderson, M. R., and Dorfmeier, C. L.: Carbonate removal from coastal sediments for the determination of organic carbon and its isotopic signatures, δ13C and Δ14C: comparison of fumigation and direct acidification by hydrochloric acid, Limnol. Oceanogr.-Meth., 6, 254–262, 2008.

Lê, S., Josse, J., and Husson, F.: FactoMineR: an R package for multivariate analysis, J. Stat. Softw., 25, 1–18, 2008.

Leithold, E. L., Blair, N. E., and Wegmann, K. W.: Source-to-sink sedimentary systems and global carbon burial: A river runs through it, Earth-Sci. Rev., 153, 30–42, 2016.

Li, Z., Peterse, F., Wu, Y., Bao, H., Eglinton, T. I., and Zhang, J.: Sources of organic matter in Changjiang (Yangtze River) bed sediments: preliminary insights from organic geochemical proxies, Org. Geochem., 85, 11–21, 2015.

Lupker, M., France-Lanord, C., Lavé, J., Bouchez, J., Galy, V., Métivier, F., Gaillardet, J., Lartiges, B., and Mugnier, J.: A Rouse-based method to integrate the chemical composition of river sediments: application to the Ganga basin, J. Geophys. Res. Earth, 116, 1–24, 2011.

Manikyamba, C., Ganguly, S., Santosh, M., Saha, A., and Lakshminarayana, G.: Geochemistry and petrogenesis of Rajahmundry trap basalts of Krishna-Godavari Basin, India, Geosci. Front., 6, 437–451, 2015.

Märki, L., Lupker, M., Gajurel, A. P., Gies, H., Haghipour, N., Gallen, S., France-Lanord, C., Lavé, J., and Eglinton, T.: Molecular tracing of riverine soil organic matter from the Central Himalaya, Geophys. Res. Lett., 47, 1–10, 2020.

Martínez-Sosa, P. and Tierney, J. E.: Lacustrine brGDGT response to microcosm and mesocosm incubations, Org. Geochem., 127, 12–22, 2019.

Martínez-Sosa, P., Tierney, J. E., and Meredith, L. K.: Controlled lacustrine microcosms show a brGDGT response to environmental perturbations, Org. Geochem., 145, 104041, https://doi.org/10.1016/j.orggeochem.2020.104041, 2020.

Mayer, L. M.: Surface area control of organic carbon accumulation in continental shelf sediments, Geochim. Cosmochim. Ac., 58, 1271–1284, 1994.

Mazumdar, A., Kocherla, M., Carvalho, M. A., Peketi, A., Joshi, R. K., Mahalaxmi, P., Joao, H. M., and Jisha, R.: Geochemical characterization of the Krishna-Godavari and Mahanadi offshore basin (Bay of Bengal) sediments: a comparative study of provenance, Mar. Pet. Geol., 60, 18–33, 2015.

Meert, J. G., Pandit, M. K., Pradhan, V. R., Banks, J., Sirianni, R., Stroud, M., Newstead, B., and Gifford, J.: Precambrian crustal evolution of Peninsular India: a 3.0 billion year odyssey, J. Asian Earth Sci., 39, 483–515, 2010.

Menges, J., Hovius, N., Andermann, C., Lupker, M., Haghipour, N., Märki, L., and Sachse, D.: Variations in organic carbon sourcing along a trans-Himalayan river determined by a Bayesian mixing approach, Geochim. Cosmochim. Ac., 286, 159–176, 2020.

Moyen, J., Martin, H., Jayananda, M., and Auvray, B.: Late Archaean granites: a typology based on the Dharwar Craton (India), Precambrian Res., 127, 103–123, 2003.

Naafs, B. D. A., Inglis, G. N., Zheng, Y., Amesbury, M. J., Biester, H., Bindler, R., Blewett, J., Burrows, M. A., del Castillo Torres, D., Chambers, F. M., Cohen, A. D., Evershed, R. P., Feakins, S. J., Galka, M., Gallego-Sala, A., Gandois, L., Gray, D. M., Hatcher, P. G., Honorio Coronado, E. N., Hughes, P. D. M., Huguet, A., Könönen, M., Laggoun-Défarge, F., Lähteenoja, O., Lamentowicz, M., Marchant, R., McClymont, E., Pontevedra-Pombal, X., Ponton, C., Pourmand, A., Rizzutti, A. M., Rochefort, L., Schellekens, J., De Vleeschouwer, F., and Pancost, R. D.: Introducing global peat-specific temperature and pH calibrations based on brGDGT bacterial lipids, Geochim. Cosmochim. Acta 208, 285–302, 2017.

Peterse, F. and Eglinton, T. I.: Grain size associations of branched tetraether lipids in soils and riverbank sediments: Influence of hydrodynamic sorting processes, Front. Earth Sci., 5, 1–8, 2017.

Peterse, F., Kim, J., Schouten, S., Kristensen, D. K., Koç, N., and Sinninghe Damsté, J. S.: Constraints on the application of the MBT/CBT palaeothermometer at high latitude environments (Svalbard, Norway), Org. Geochem., 40, 692–699, 2009.

Peterse, F., Nicol, G. W., Schouten, S., and Sinninghe Damsté, J. S.: Influence of soil pH on the abundance and distribution of

core and intact polar lipid-derived branched GDGTs in soil, Org. Geochem. 41, 1171–1175, 2010.

Pitcher, A., Rychlik, N., Hopmans, E. C., Spieck, E., Rijpstra, W. I. C., Ossebaar, J., Schouten, S., Wagner, M, and Sinninghe Damsté, J. S.: Crenarchaeol dominates the membrane lipids of Candidatus Nitrosospheaera gargensis, a thermophilic Group I.1b Archaeon, ISME J., 4, 542–552, 2010.

Pitcher, A., Hopmans, E. C., Mosier, A. C., Park, S. J., Rhee, S. K., Fancis, C. A., Schouten, S., and Sinninghe Damsté, J. S.: Core and intact polar glycerol dibiphytanyl glycerol tetraether lipids of ammonia-oxidizing Archaea enriched from marine and estuarine sediments, Appl. Environ. Microbiol., 77, 3468–3477, 2011.

Ponton, C., Giosan, L., Eglinton, T. I., Fuller, D. Q., Johnson, J. E., Kumar, P., and Collett, T. S.: Holocene aridification of India, Geophys. Res. Lett., 39, L03704–L03709, 2012.

Pradhan, U. K., Wu, Y., Shirodkar, P. V., Zhang, J., and Zhang, G.: Multi-proxy evidence for compositional change of organic matter in the largest tropical (peninsular) river basin of India, J. Hydrol., 519, 999–1009, 2014.

Rao, K. N., Saito, Y., Nagakumar, K. C. V., Demudu, G., Rajawat, A. S., Kubo, S., and Li, Z.: Palaeogeography and evolution of the Godavari delta, east coast of India during the Holocene: an example of wave-dominated and fan-delta settings, Palaeogeogr. Palaeoclimatol. Palaeoecol., 440, 213–233, 2015.

Regnier, P., Friedlingstein, P., Ciais, P., Mackenzie, F. T., Gruber, N., Janssens, I. A., Laruelle, G. G., Lauerwald, R., Luyssaert, S., and Andersson, A. J.: Anthropogenic perturbation of the carbon fluxes from land to ocean, Nat. Geosci., 6, 597–607, 2013.

Sarma, V., Paul, Y. S., Vani, D. G., and Murty, V.: Impact of river discharge on the coastal water pH and pCO_2 levels during the Indian Ocean Dipole (IOD) years in the western Bay of Bengal, Cont. Shelf Res., 107, 132–140, 2015.

Schouten, S., Huguet, C., Hopmans, E. C., Kienhuis, M. V., and Sinninghe Damsté, J. S.: Analytical methodology for TEX86 paleothermometry by high-performance liquid chromatography/atmospheric pressure chemical ionization-mass spectrometry, Anal. Chem., 79, 2940–2944, 2007.

Singh, P. K., Singh, M. P., Prachiti, P. K., Kalpana, M. S., Manikyamba, C., Lakshminarayana, G., Singh, A. K., and Naik, A. S.: Petrographic characteristics and carbon isotopic composition of Permian coal: Implications on depositional environment of Sattupalli coalfield, Godavari Valley, India, Int. J. Coal Geol., 90–91, 34–42, 2012.

Sinninghe Damsté, J. S.: Spatial heterogeneity of sources of branched tetraethers in shelf systems: The geochemistry of tetraethers in the Berau River delta (Kalimantan, Indonesia), Geochim. Cosmochim. Ac., 186, 13–31, 2016.

Sinninghe Damsté, J. S., Schouten, S., Hopmans, E. C., Van Duin, A. C., and Geenevasen, J. A.: Crenarchaeol, J. Lipid Res., 43, 1641–1651, 2002.

Sinninghe Damsté, J. S., Rijpstra, W. I. C., Hopmans, E. C., Weijers, J. W., Foesel, B. U., Overmann, J., and Dedysh, S. N.: 13, 16-Dimethyl octacosanedioic acid (iso-diabolic acid), a common membrane-spanning lipid of Acidobacteria subdivisions 1 and 3, Appl. Environ. Microbiol., 77, 4147–4154, 2011.

Sinninghe Damsté, J. S., Rijpstra, W. I. C., Hopmans, E. C., Jung, M. Y., Kim, J. G., Rhee, S. K., Stieglmeier, M., and Schleper, C.: Intact polar and core glycerol dibiphytanyl glycerol tetraether lipids of group I.1a and I.1b Thaumarchaeota in soil, Appl. Environ. Microbiol. 78, 6866–6874, 2012.

Sinninghe Damsté, J. S., Rijpstra, W. I. C., Hopmans, E. C., Foesel, B. U., Wüst, P. K., Overmann, J., Tank, M., Bryant, D. A., Dunfield, P. F., and Houghton, K.: Ether-and ester-bound iso-diabolic acid and other lipids in members of Acidobacteria subdivision 4, Appl. Environ. Microbiol., 80, 5207–5218, 2014.

Sinninghe Damsté, J. S., Rijpstra, W. I. C., Foesel, B. U., Huber, K. J., Overmann, J., Nakagawa, S., Kim, J. J., Dunfield, P. F., Dedysh, S. N., and Villanueva, L.: An overview of the occurrence of ether-and ester-linked iso-diabolic acid membrane lipids in microbial cultures of the Acidobacteria: Implications for brGDGT paleoproxies for temperature and pH, Org. Geochem., 124, 63–76, 2018.

Sparkes, R. B., Doğrul Selver, A., Bischoff, J., Talbot, H. M., Gustafsson, Ö., Semiletov, I. P., Dudarev, O. V., and van Dongen, B. E.: GDGT distributions on the East Siberian Arctic Shelf: implications for organic carbon export, burial and degradation, Biogeosciences, 12, 3753–3768, https://doi.org/10.5194/bg-12-3753-2015, 2015.

Sridhar, P. N., Ali, M. M., Vethamony, P., Babu, M. T., Ramana, I. V., and Jayakumar, S.: Seasonal occurrence of unique sediment plume in the Bay of Bengal, Eos, 89, 22–23, 2008.

Stuut, J. W., Kasten, S., Lamy, F., and Hebbeln, D.: Sources and modes of terrigenous sediment input to the Chilean continental slope, Quat. Int, 161, 67–76, 2007.

Sun, S., Schefuß, E., Mulitza, S., Chiessi, C. M., Sawakuchi, A. O., Zabel, M., Baker, P. A., Hefter, J., and Mollenhauer, G.: Origin and processing of terrestrial organic carbon in the Amazon system: lignin phenols in river, shelf, and fan sediments, Biogeosciences, 14, 2495–2512, https://doi.org/10.5194/bg-14-2495-2017, 2017.

Syvitski, J. P. and Saito, Y.: Morphodynamics of deltas under the influence of humans, Global Planet. Change, 57, 261–282, 2007.

Tao, S., Eglinton, T. I., Montluçon, D. B., McIntyre, C., and Zhao, M.: Pre-aged soil organic carbon as a major component of the Yellow River suspended load: Regional significance and global relevance, Earth Planet. Sci. Lett., 414, 77–86, 2015.

Usman, M. O., Kirkels, F. M. S. A., Zwart, H. M., Basu, S., Ponton, C., Blattmann, T. M., Ploetze, M., Haghipour, N., McIntyre, C., Peterse, F., Lupker, M., Giosan, L., and Eglinton, T. I.: Reconciling drainage and receiving basin signatures of the Godavari River system, Biogeosciences, 15, 3357–3375, https://doi.org/10.5194/bg-15-3357-2018, 2018.

van der Voort, T. S., Hagedorn, F., McIntyre, C., Zell, C., Walthert, L., Schleppi, P., Feng, X., and Eglinton, T. I.: Variability in ^{14}C contents of soil organic matter at the plot and regional scale across climatic and geologic gradients, Biogeosciences, 13, 3427–3439, https://doi.org/10.5194/bg-13-3427-2016, 2016.

van Soelen, E. E., Kim, J., Santos, R. V., Dantas, E. L., de Almeida, F. V., Pires, J. P., Roddaz, M., and Sinninghe Damsté, J. S.: A 30 Ma history of the Amazon River inferred from terrigenous sediments and organic matter on the Ceará Rise, Earth Planet. Sci. Lett., 474, 40–48, 2017.

Vonk, J. E., van Dongen, B. E., and Gustafsson, Ö: Lipid biomarker investigation of the origin and diagenetic state of sub-arctic terrestrial organic matter presently exported into the northern Bothnian Bay, Mar. Chem., 112, 1–10, 2008.

Vonk, J. E., Sánchez-García, L., Semiletov, I., Dudarev, O., Eglinton, T., Andersson, A., and Gustafsson, Ö.: Molecular and radiocarbon constraints on sources and degradation of terrestrial organic carbon along the Kolyma paleoriver transect, East Siberian Sea, Biogeosciences, 7, 3153–3166, https://doi.org/10.5194/bg-7-3153-2010, 2010.

Warden, L., Kim, J.-H., Zell, C., Vis, G.-J., de Stigter, H., Bonnin, J., and Sinninghe Damsté, J. S.: Examining the provenance of branched GDGTs in the Tagus River drainage basin and its outflow into the Atlantic Ocean over the Holocene to determine their usefulness for paleoclimate applications, Biogeosciences, 13, 5719–5738, https://doi.org/10.5194/bg-13-5719-2016, 2016.

Warden, L., Moros, M., Weber, Y., and Sinninghe Damsté, J. S.: Change in provenance of branched glycerol dialkyl glycerol tetraethers over the Holocene in the Baltic Sea and its impact on continental climate reconstruction, Org. Geochem., 121, 138–154, 2018.

Ward, N. D., Bianchi, T. S., Medeiros, P. M., Seidel, M., Richey, J. E., Keil, R. G., and Sawakuchi, H. O.: Where carbon goes when water flows: carbon cycling across the aquatic continuum, Front. Mar. Sci., 4, 1–27, 2017.

Weijers, J. W., Schouten, S., Hopmans, E. C., Geenevasen, J. A., David, O. R., Coleman, J. M., Pancost, R. D., and Sinninghe Damsté, J. S.: Membrane lipids of mesophilic anaerobic bacteria thriving in peats have typical archaeal traits, Environ. Microbiol., 8, 648–657, 2006.

Weijers, J. W., Schouten, S., van den Donker, Jurgen C, Hopmans, E. C., and Sinninghe Damsté, J. S.: Environmental controls on bacterial tetraether membrane lipid distribution in soils, Geochim. Cosmochim. Ac., 71, 703–713, 2007a.

Weijers, J. W., Schefuß, E., Schouten, S., and Sinninghe Damsté, J. S.: Coupled thermal and hydrological evolution of tropical Africa over the last deglaciation, Science, 315, 1701–1704, 2007b.

Weijers, J. W., Schouten, S., Schefuß, E., Schneider, R. R., and Sinninghe Damsté, J. S.: Disentangling marine, soil and plant organic carbon contributions to continental margin sediments: a multi-proxy approach in a 20,000 year sediment record from the Congo deep-sea fan, Geochim. Cosmochim. Ac., 73, 119–132, 2009a.

Weijers, J. W., Panoto, E., van Bleijswijk, J., Schouten, S., Rijpstra, W. I. C., Balk, M., Stams, A. J., and Sinninghe Damsté, J. S.: Constraints on the biological source (s) of the orphan branched tetraether membrane lipids, Geomicrobiol. J., 26, 402–414, 2009b.

WRB FAO (World Reference Base for Soil Resources, Food and Agriculture Organisation of the United Nations): IUSS Working Group WRB, World Reference Base for Soil Resources 2014, update 2015 International soil classification system for naming soils and creating legends for soil maps, World Soil Resources Reports No. 106. FAO, Rome, Italy, ISBN: 978-92-5-108369-7, 2015.

Xiao, W., Wang, Y., Zhou, S., Hu, L., Yang, H., and Xu, Y.: Ubiquitous production of branched glycerol dialkyl glycerol tetraethers (brGDGTs) in global marine environments: a new source indicator for brGDGTs, Biogeosciences, 13, 5883–5894, https://doi.org/10.5194/bg-13-5883-2016, 2016.

Xiao, W., Wang, Y., Liu, Y., Zhang, X., Shi, L., and Xu, Y.: Predominance of hexamethylated 6-methyl branched glycerol dialkyl glycerol tetraethers in the Mariana Trench: source and environmental implication, Biogeosciences, 17, 2135–2148, https://doi.org/10.5194/bg-17-2135-2020, 2020.

Xie, S., Pancost, R. D., Chen, L., Evershed, R. P., Yang, H., Zhang, K., Huang, J., and Xu, Y.: Microbial lipid records of highly alkaline deposits and enhanced aridity associated with significant uplift of the Tibetan Plateau in the Late Miocene, Geology, 40, 291–294, 2012.

Xu, Y., Jia, Z., Xiao, W., Fang, J., Wang, Y., Luo, M., Wenzhöfer, F., Rowden, A. A., and Glud, R. N.: Glycerol dialkyl glycerol tetraethers in surface sediments from three Pacific trenches: Distribution, source and environmental implications, Org. Geochem., 147, 1–12, 2020.

Yang, G., Zhang, C. L., Xie, S., Chen, Z., Gao, M., Ge, Z., and Yang, Z.: Microbial glycerol dialkyl glycerol tetraethers from river water and soil near the Three Gorges Dam on the Yangtze River, Org. Geochem., 56, 40–50, 2013.

Yang, H., Pancost, R. D., Dang, X., Zhou, X., Evershed, R. P., Xiao, G., Tang, C., Gao, L., Guo, Z., and Xie, S.: Correlations between microbial tetraether lipids and environmental variables in Chinese soils: Optimizing the paleo-reconstructions in semi-arid and arid regions, Geochim. Cosmochim. Ac., 126, 49–69, 2014.

Yatagai, A., Kamiguchi, K., Arakawa, O., Hamada, A., Yasutomi, N., and Kitoh, A.: APHRODITE: Constructing a long-term daily gridded precipitation dataset for Asia based on a dense network of rain gauges, B. Am. Meteorol. Soc., 93, 1401–1415, 2012.

Zell, C., Kim, J., Abril, G., Sobrinho, R., Dorhout, D., Moreira-Turcq, P., and Sinninghe Damsté, J.: Impact of seasonal hydrological variation on the distributions of tetraether lipids along the Amazon River in the central Amazon basin: implications for the MBT/CBT paleothermometer and the BIT index, Front. Microbiol., 4, 1–14, 2013a.

Zell, C., Kim, J., Moreira-Turcq, P., Abril, G., Hopmans, E. C., Bonnet, M., Sobrinho, R. L., and Sinninghe Damsté, J. S.: Disentangling the origins of branched tetraether lipids and crenarchaeol in the lower Amazon River: Implications for GDGT-based proxies, Limnol. Oceanogr., 58, 343–353, 2013b.

Zell, C., Kim, J.-H., Balsinha, M., Dorhout, D., Fernandes, C., Baas, M., and Sinninghe Damsté, J. S.: Transport of branched tetraether lipids from the Tagus River basin to the coastal ocean of the Portuguese margin: consequences for the interpretation of the MBT′/ CBT paleothermometer, Biogeosciences, 11, 5637–5655, https://doi.org/10.5194/bg-11-5637-2014, 2014a.

Zell, C., Kim, J., Hollander, D., Lorenzoni, L., Baker, P., Silva, C. G., Nittrouer, C., and Sinninghe Damsté, J. S.: Sources and distributions of branched and isoprenoid tetraether lipids on the Amazon shelf and fan: Implications for the use of GDGT-based proxies in marine sediments, Geochim. Cosmochim. Ac., 139, 293–312, 2014b.

Zell, C., Kim, J., Dorhout, D., Baas, M., and Sinninghe Damsté, J. S.: Sources and distributions of branched tetraether lipids and crenarchaeol along the Portuguese continental margin: Implications for the BIT index, Cont. Shelf Res., 96, 34–44, 2015.

Zhu, C., Weijers, J. W., Wagner, T., Pan, J., Chen, J., and Pancost, R. D.: Sources and distributions of tetraether lipids in surface sediments across a large river-dominated continental margin, Org. Geochem., 42, 376–386, 2011.